AD-A145 957   COMPUTATIONAL KINETICS AND SENSITIVITY ANALYSIS OF   1/1
               HYDROGEN-OXYGEN COMBUSTION(U) PRINCETON UNIV NJ DEPT OF
               CHEMISTRY   E P DOUGHERTY ET AL. 1982 N00014-82-K-2068

UNCLASSIFIED   F/G 21/2   NL
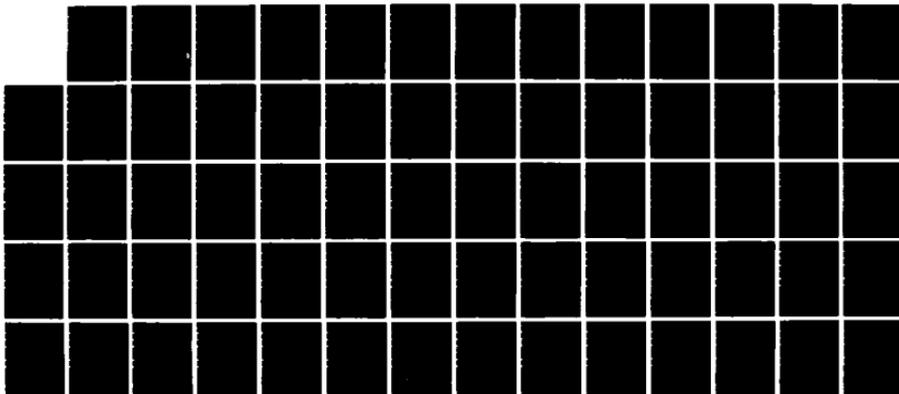
END
FILMED
DTIC
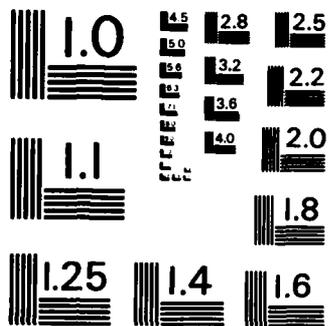
MICROCOPY RESOLUTION TEST CHART

NATIONAL BUREAU OF STANDARDS-1963-A

Computational Kinetics and

Sensitivity Analysis of

Hydrogen-Oxygen Combustion

Eugene P. Dougherty[†] and Herschel Rabitz[‡]

Department of Chemistry

Princeton University

Princeton, New Jersey 08544

N00014-82-K-2068

[†] Present address: Research Laboratories

Rohm and Haas Company

Spring House, Pennsylvania 19477

[‡] Alfred P. Sloan Fellow and Camille and Henry Dreyfus Teacher-Scholar.

84 08 08 001

Abstract

Kinetic modeling calculations on the H_2-O_2 system have been carried out with an extensive reaction set to probe the vicinity of the three explosion limits. Sensitivity analysis is used throughout this investigation to study system behavior, in particular, to elucidate mechanistic details. The concentrations and sensitivity profiles are discussed in light of the appropriate experimental results and existing theories of hydrogen combustion. The results indicate the present model to be useful over a wide pressure-temperature range. The reaction set is also used to probe the sensitivities for an experimental study designed to measure the rate constant of an important elementary reaction, $H + O_2 + M \longrightarrow HO_2 + M$, involved in this system. The versatility of the reaction set is also demonstrated by a study of a related chemical reaction, the decomposition of hydrogen peroxide. Finally, prospects for utilizing the methods and results of this study to examine other complex kinetic schemes are discussed.

Accession For

NTIS GRA&I

DTIC TAB

Unannounced

Justification

By

Distribution

Availability Codes

Dist | Avail and/or Special

A-1

I. Introduction

Numerical modeling is becoming a valuable tool in elucidating the behavior of large and complex systems in fields as diverse as reaction kinetics,[1] operations research,[2] world models for population and resources,[3] and mathematical biology.[4] Modeling has been shown to be of particular importance in investigating the details of complex combustion processes.[5] In this work we present a model developed to investigate the kinetics of a simple combustion process,

$$H_2(g) \ + \ \tfrac{1}{2}O_2(g) \ \longrightarrow \ H_2O(g)$$
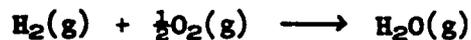
We present the results of detailed numerical calculations involving the proposed mechanism for this system over a wide range of temperatures and pressures. These calculations contribute to an understanding of this well-studied intriguing combustion reaction.

This study of the H_2-O_2 system differs in certain respects from similar numerical studies on complex kinetic schemes[6] because sensitivity analysis plays a dominant role.[7] In any numerical study it is desirable to understand how sensitive the system solutions are to the various input parameters of the model. Generally most numerical studies of complex systems probe sensitivities via the "brute force" technique of changing parameters and observing the effects upon the output solutions. However, recently in the field of chemical kinetics, several more systematic and economical approaches to sensitivity analysis have been developed.[8-14] In particular, the Green's Function Method (GFM)[13] has already been shown to be a useful and competitive approach to the problem of sensitivity analysis in chemical kinetics[14] as well as in quantum

dynamics.[15] The present paper provides an application of sensitivity analysis utilizing the GFM to deduce information regarding explosion limits, mechanistic details, etc., for the H_2-O_2 system.

In brief, then, this work investigates what we believe to be a realistic model for hydrogen combustion by means of a detailed analysis of concentrations and sensitivity profiles. An attempt is made to identify and understand the somewhat enigmatic temperature-pressure behavior of this system, the important mechanistic pathways and the critical rate constants for the process. The numerical results - concentrations and sensitivities - are discussed in light of relevant experiments and models. The utility of sensitivity analysis and kinetic modeling is apparent by suggestions from this work for additional experiments to understand this important system more thoroughly. Finally, the reaction set developed for the H_2-O_2 system is shown to be versatile enough to analyze sensitivities in an experimental study of an important elementary step $H + O_2 + M \longrightarrow HO_2 + M$ of the model. Calculations have also been carried out to probe a related chemical reaction, the decomposition of hydrogen peroxide.

The paper is divided into six remaining sections. Section II provides a brief introduction to the H_2-O_2 system and discusses the development of the reaction model. Section III discusses some computational details for this system. Section IV is a detailed analysis of the results of many calculations, focusing upon system behavior at the three explosion limits for the reaction. Section V is an analysis of sensitivities for an experimental probe of the $H + O_2 + M \longrightarrow HO_2 + M$ step in the model. Section VI discusses the results of calculations for the decomposition of H_2O_2. Finally, Section VII provides

a discussion of the methods and results, and suggests future possibilities

for research.

II. An Introduction to the H_2-O_2 System

The formation of H_2O from H_2 and O_2 has been the subject of hundreds of papers and is still a problem for active research. At room temperatures and ordinary pressures, the reaction is very slow. When the mixture is heated and subjected to a spark or an activating surface, however, the process can be very rapid, even explosive. Particularly interesting behavior occurs in the temperature range $650 - 850°K$ for reactant pressures of 1 to 5,000 torr. Figures 1 and 2 illustrate some peculiarities in the behavior of a stoichiometric mixture of H_2 and O_2. The so-called first, second and third explosion limits are shown. Explosion limits are not, strictly speaking, flammability limits. They are the pressure-temperature boundaries for a specific mixture of fuel and oxidizer that separate the regions of slow and fast reactions.[16] In the explosive regime flames can be supported via steady diffusional mechanisms. Many experiments have been carried out to probe the effects of vessel size, vessel composition, surface composition, inert gases, etc., on these three limits. Although these experiments are described in considerable detail in several texts,[17-22] a brief summary of the results for each explosion limit is appropriate.

Below the first explosion limit the reaction proceeds almost negligibly slowly. However, if a stoichiometric mixture of H_2 and O_2 is added slowly to a reaction vessel, the mixture experiences a mild explosion near a few torr. The pressure is defined as the sum of the initial partial pressures of H_2 and O_2. The first limit boundaries between the regions of slow and fast reaction, is quite dependent upon vessel size and vessel composition. Frost and Alyea[23] found that rinsing their vessels with KCl

raised the limit pressure to several times higher than previously. The marked dependence upon vessel size and vessel composition indicates that diffusional mechanisms are very important in this regime. There is competition between the formation of radicals which undergo chain reactions and the destruction of such chains via migration to the walls of the vessel.

The neighborhood of the second explosion limit has been probed by both the heating method, in which a mixture of H_2 and O_2, initially in the nonexplosive regime between the second and third limits, is heated until an explosion is observed, and by the withdrawal method, in which slow evacuation of the mixture is carried out until explosion occurs.[21] The experimental evidence indicates that behavior in the neighborhood of the second explosion limit must be explained by gas phase production and destruction of radicals.[16] Evidently, diffusion plays a less dominant role than it does for the first explosion limit, since the second limit pressure is independent of the vessel size, provided its volume is sufficiently large.[17] Still, there is some dependence upon the composition of the surface, that is, different kinetic behavior is observed for uncoated surfaces and those coated with salt or acid.[17] This indicates the important role played by the surface in the initiation and, to a lesser extent, destruction of gas phase radicals. Once produced, the production of these radicals is accelerated by chain branching reactions such as $H + O_2 \longrightarrow OH + O$, resulting in very rapid reaction. The slow reaction at higher pressures is usually explained by a third order non-branching reaction which overtakes the $H + O_2 \longrightarrow OH + O$ step.[16] Although some investigators have attempted to describe the second limit without recourse to the metastable HO_2 radical[21,24], it is now

generally accepted that the important third order reaction is

$$H + O_2 + M \longrightarrow HO_2 + M$$

The characteristic slow reaction at pressures between the second and third limits proceeds through the formation of the hydroperoxyl radical and hydrogen peroxide, which has been observed experimentally in this regime.[25]

At the first and second limits, the observed explosions are of the isothermal branched-chain type, and just outside the limits the overall reaction rate is extremely small.[21] At the third limit, however, there is no such sharp transition from slow reaction to explosion, and the reaction rate is high even below the limit.[17] For this reason it has not been established whether the third limit has mainly a chain or a thermal character. Potassium chloride wall coating hinders the explosion, suggesting that chains are involved. Careful studies of the third limit are difficult because of technical problems in handling the reactants and determining their pressures prior to the onset of a very rapid reaction. The explosion is thought to be due to a combination of chain and thermal mechanisms, that is to say, the heat given out by the chain reactions cannot be dissipated sufficiently rapidly, so that self-heating occurs, followed by explosion.[22] Glassman[16] suggests that the third limit is due to a reaction that overtakes the stability of the HO_2, most possibly the reaction

$$HO_2 + H_2 \longrightarrow H_2O_2 + H$$
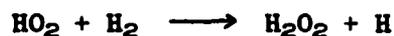
which regenerates a large number of active particles. Lewis and Von Elbe[21] have carried out some experiments near the curve joining the second and third

explosion limits. One experiment investigates a stoichiometric mixture of H_2 and O_2 in N_2 initially at $847°K$ and 300 torr, for which the initial reaction rate (rate when $\sim 10\%$ of the H_2O has been formed) is about 1.5 torr/min. In this case no explosion occurs, as the rate is too small to seriously disturb isothermal conditions: the heat is rapidly dissipated. However, at $823°K$ and 950 torr, the initial rate is 20 - 40 torr/min, which is sufficiently large to raise the temperature and then cause explosion after a very short induction period. This particular experiment is described in considerable detail, since very reliable experimental results are lacking in this regime because of the difficulties we have cited. The computational results described in Section IV will shed some light on kinetic behavior in this regime.

There have been many attempts to explain the complicated pressure-temperature behavior of this system by various models. Some models include very few reactions and attempt to include diffusional mechanisms, heat release, etc.[26] Others have focused primarily upon mass action kinetics. Baldwin, et al.,[27] have constructed a reaction set which is representative of the types of kinetic mechanisms that have been considered.

In building the reaction set for this paper, we have assumed a conservative posture by including virtually every conceivable reaction which might be important that involves the species H_2, O_2, H_2O, H_2O_2, HO_2, H, O, and OH. All these species have been positively identified in hydrogen flames, although reactions involving ozone are often excluded, since its concentration rarely exceeds a few ppm.[28] The present authors have carried out an extensive literature search of several data bases to construct the reaction set and to

obtain the best possible numerical values available for the rate constant parameters for the elementary steps of the mechanism. The literature values have been carefully reviewed and values assigned based upon the authors' evaluations regarding which measurements and/or estimates are the most accurate. The results of this effort are embodied in Table I, which lists each reaction with appropriate rate constant parameters and uncertainties. The reaction set of Baldwin, et al.,[27] is also indicated in this table. In general the rate constants are of a modified Arrhenius form, i.e.,

$$k_i = A_i T^{B_i} \exp(-C_i/T) \qquad (2.1)$$

Most of the calculations described in the following sections of this paper utilize the first 57 reactions of Table I. The wall reactions (58 - 62) have been included in the mechanism to probe wall effects in the vicinity of the first and second limits. Of course, the numerical values of these wall reaction rate constants varies with the vessel surface-to-volume ratio, its composition, the method of preparation, etc. Thus we have chosen values from the literature[84,85] corresponding to values for typical laboratory conditions to merely simulate wall effects.

Several adiabatic calculations were carried out in the region of the third (thermal) explosion limit. These calculations required the specific enthalpy (h_i) and the specific heat capacity (C_{v_i}) for each species. For the purposes of these calculations both h_i and C_{v_i} are adequately represented as linear functions of temperature in the range of interest (500 - 6000°K). Linear least squares fits to the tabulated JANAF data[66] were used to obtain the coefficients listed in Table II.

III. A Sample Calculation for the H_2-O_2 System

The purpose of this section is to explain the numerics of a single calculation in considerable detail in order to show how the computations are carried out, what sort of information is obtained, what error tolerances are used, etc. Detailed discussions of kinetic and sensitivity results are given in Sections IV, V and VI.

The formulation and numerical considerations of the Green's Function Method of sensitivity analysis have already been treated in two other papers.[13],[14] Briefly, to determine concentrations and sensitivity profiles, one must first solve the initial value problem resulting from the application of the law of mass action[67] to reaction mechanisms. The resulting (generally stiff) differential equations are of the form

$$\frac{d}{dt} \underline{y} = \underline{f}(\underline{y}, \underline{\alpha}, t) \quad , \quad \underline{y}(0) = \underline{y}^{(0)} \tag{3.1}$$

where $\underline{y}$ denotes an n-vector of species concentrations, $\underline{\alpha}$ is an m-vector of system parameters (i.e., rate constants and initial concentrations), t refers to time and $\underline{f}$ is a nonlinear function of the concentrations. Once the n concentration profiles have been obtained, the sensitivities are determined by solving n sets of n-dimensional ordinary differential equations for the adjoint Green's function matrix. In the course of solving these equations, the mesh chosen automatically by the differential equation solver[68] is used as a guide to construct the grid required to evaluate the integrals for the sensitivity coefficients $\frac{\partial y_i}{\partial \alpha_j}(t)$. The normalized sensitivity coefficients $\frac{\partial \ln y_i}{\partial \ln \alpha_j}(t)$ are especially useful measures of how sensitive a particular

species concentration is to a particular parameter. In subsequent sections we will explain how these sensitivities may be used to study system behavior.

The sample calculation described here has been carried out at a constant temperature of $700°K$. The initial pressure is 320 torr, the reactants H_2 and O_2 are initially in a stoichiometric ratio and no diluent is present. This situation corresponds to the nonexplosive regime between the second and third limits. Only the first 57 reactions of Table I are used in this calculation. All calculations described in this paper are performed in double precision on an IBM 360/91 computer. The error tolerance $\mathcal{E} = 10^{-3}$ was used in solving the differential equations, although occasionally a stricter tolerance was used to check precision.

The differential equations for the concentrations were solved first, and the results are displayed graphically in Figure 3. This behavior is fairly typical of the qualitative features expected and observed for the slow regime between the second and third limits. This regime will be considered more fully in Section IV. The differential equations for this problem are very stiff; the stiffness ratio - the ratio of the largest (in magnitude) to smallest eigenvalue - is typically $\sim 10^{10} - 10^{11}$, yet still only a few hundred steps are required by the ODE solver to reach 90% reaction completion. In the course of computing the concentrations, various terms contributing to f_i, which are of the form $\pm k_j y_k y_\ell$, are computed and printed at selected times. This is useful in screening analysis,[28] which assigns the importance of reaction rate constants based upon the magnitude of the individual reaction contributions to total species derivatives. Mass conservation relations[14] are also checked and verified at several times.

For the sensitivities, the differential equations for each row of the adjoint Green's function matrix have to be solved. This requires an interpolation grid for the concentration vector $\underline{y}$. Relatively coarse grids (~ 50 grid points) are sufficient to obtain reasonable precision. Each of the n rows of the adjoint Green's function matrix - corresponding to the n species present - require as many as several thousand or as few as twenty steps by the differential equation solver to obtain sensitivities at a particular time. Sensitivities are obtained at four separate times. The stiff nature of this system is exhibited in the boundary layer behavior for the typical sensitivity integrals. This type of behavior has already been documented for a previous study.[14] As Figure 4 shows, the integral is generally determined by only a very small portion of the integrand. Since the exponential option for numerical quadrature[14] is employed, and since the mesh chosen by the solver is used to construct the integration grid (in this study every third mesh point is utilized), the results should be quite accurate. The sensitivity mass conservation relations described in reference 14 are reasonably well satisfied.

The final point concerns computational time estimates. To obtain concentrations at a reasonably fine grid of times for up to 90% reaction completion requires about three seconds of execution time on the IBM 360/91 computer. The adiabatic calculations described later in the paper require about twenty seconds. To obtain sensitivities for a single species with respect to all parameters at a single time requires only a few more seconds, depending upon which species. The times are essentially independent of the number of parameters considered. Generally, it was found desirable to obtain

sensitivities for all species at least four times during the reaction for this and most of the other calculations. Since occasionally the solver takes thousands of steps for one species, the total execution time is about 2.1 minutes, which is fairly typical for most of the calculations. Based upon previous studies,[14] it is expected that the direct method of sensitivity analysis[8-10] would take at least twenty minutes of execution time to obtain similar sensitivity information. Unfortunately we have been unable to implement the direct method successfully for this reaction set, presumably because of numerical difficulties, so this estimate may be subject to some error. The Fourier Amplitude Sensitivity Test,[11,12] which defines sensitivities in a somewhat different fashion by averaging over the uncertainties of other parameters in the model, would require ~30,000 kinetic runs for a 57 parameter system for fourth-order interferences according to a formula given by its authors.[69]

IV. Detailed Results of the H_2-O_2 Calculations

The results described in this section are for calculations of the same type as that described in the previous section. That is to say, the same error tolerances, integration procedures, etc., were used, and similar numerical behavior was observed. Any exceptions are specifically noted. In these calculations the regions around each of the three explosion limits are given particular attention. The effects of inert gas diluents, mixture composition, temperature and pressure on the behavior in the vicinity of these limits were also investigated. Mechanistic details were probed chiefly by sensitivity analysis.

As a preview to this section, consider Figure 5, which displays the results of several kinetic calculations in the vicinity of the three limits. The qualitative and some quantitative features observed in experimental studies[16-23] are also evident in these modeling results, as indicated by the trends in the calculated kinetic behavior shown in Figure 5. The reproduction of these features attests to the validity of the reaction mechanism and the calculations.

A. The first explosion limit.

In the region just above and below the first limit pressure, diffusion appears to be an important part of the mechanism. In this regard the limitations of our model are evident. To assess the effects of diffusion, calculations are often carried out with and without the wall reactions (58 - 62). The assumption is that wall reactions and diffusional mechanisms achieve a similar result: destruction of radical species before the reaction is

completed. The general validity of this assumption is doubtful (e.g., no account is allowed for the surface-to-volume ratio in the wall reaction model). Nevertheless, wall reactions are included to test their effects.

First consider a calculation carried out at $750^\circ K$ at an initial pressure of 3.2 torr, consisting only of the reactants H_2 and O_2 present in a stoichiometric ratio. A large concentration of radicals, particularly H, develops rather quickly after a short induction period of 1 sec, immediately followed by an explosion. Sensitivities of [H] to the rate constants were probed at 0.15 seconds. Here and in further discussions of sensitivities use is made of the notation a(b), where a refers to the reaction number of Table I whose rate constant is considered, and b is the numerical value of the relevant normalized sensitivity coefficient. The sensitivities are generally rank-ordered according to magnitude. The results for [H] sensitivities are

$$11(17) > 20(1.4) > 35(1.0) > 12(-0.7) > 26(0.1)$$

Other important reactions include 2, 3, 4 and 24. Reaction 35 is a chain-initiator, while the other reactions involve chain-branching, chain-propagation and chain-termination. The large sensitivity of Reaction 11 $(H + O_2 \longrightarrow OH + O)$ indicates the importance of chain-branching in this run. If the sensitivity to reaction 12 $(H + O_2 + M \longrightarrow HO_2 + M)$ were larger, a slower, less explosive reaction would be indicated. As we shall see later, the branching ratio $R_B = k_{11}/k_{12} M$, obtained from a simple stability theory, is an important leading indicator of whether or not explosion will occur.[21,70] In this case $R_B \cong 1$, indicating an explosion. When the calculations are

repeated including the wall reactions (58 - 62), the overall rate is about a factor of three slower, as the reactive radical species are destroyed. While we have chosen literature values of the wall reactions corresponding to typical situations, it is true that certain types of walls can promote radical formation rather than inhibiting it. Sensitivities to the wall reactions involving H and O (reactions 60 and 61) were quite large. Other than these effects, the wall reactions change the major features of the kinetic behavior very little: a chain mechanism involving virtually the same set of reactions is still suggested by the sensitivity results. A third calculation was carried out with the same initial conditions except that 700 torr of argon was present as a diluent. In this case the reaction rate increases quite substantially. This effect is consistent with the experimental result[17,21] that increased inert gas pressure causes a lowering of the first explosion limit pressure (initial pressure of the H_2 and O_2 reactants). This pressure lowering is generally explained[17] by the argument that the presence of inert gas hinders diffusion of radicals to the wall and hence promotes rapid reaction. It is especially interesting that the present kinetic calculations indicate an increased rate, since the presence of argon might be expected to inhibit a branched-chain explosion due to the increase in [M] which decreases R_B.

The effect of reactant pressures was also investigated. At 750°K with H_2/O_2 present in a stoichiometric ratio and no diluent we carried out calculations at reactant pressures from 32 torr down to $\lesssim 0.1$ torr. At the lowest pressures the reaction is almost three orders of magnitude slower than for the highest pressures. Over the entire pressure range essentially

the same set of reactions were important. This indicates that a chain mechanism persists, yet if diffusion were included in the model, it is likely that the chain would never propagate to any appreciable extent. With regard to initial pressures, we obtain the result that virtually all species concentrations are about an order of magnitude more sensitive to the initial concentration of O_2 than to that of H_2 in this regime. This result likely reflects (again!) the importance of reaction 11, which directly involves O_2 but not H_2.

The effect of temperature was also studied. As indicated by the experiments,[17,21] the first limit pressure has a mild temperature dependence. The calculations indicated the first limit pressure to be about 1 torr or so in the $750 - 850^\circ$K regime. The overall reaction rate did not change very much, and the chain mechanism persists. The effects of including wall reactions in the mechanism as well as the effects of the presence of an inert gas were similar to those described earlier. On the other hand, at slightly lower temperatures, particularly where the first and second limits coalesce, some dramatic changes are observed. For example, at 730°K and an initial reactant pressure of 6 torr, a fast, explosive reaction was observed. At 650°K for the 6 torr initial reactant pressure, a somewhat slower, yet still explosive, reaction is indicated. However, at 720°K and an initial reactant pressure of 14 torr, a very slow nonexplosive reaction results, dominated by the presence of HO_2 and H_2O_2, rather than H, O and OH.

B.   The second explosion limit.

There have been many experimental studies of the second explosion limit and the slow reaction between the second and third limits. Part of the reason for this interest is that chemical kinetics rather than fluid dynamics is expected to dominate the process. Still, the quantitative experimental results obtained for the limit pressures are dependent upon the vessel composition and the method of preparation of the reaction vessel. For this reason the present discussion of the effects of temperature, pressure and inert diluents is largely qualitative.

Several calculations were performed at 320 torr for a stoichiometric ratio of reactants from temperatures in the range 400 - 1600°K. The reaction is negligibly slow at room temperature for this pressure regime. Figure 3, which shows the concentration profiles for the sample calculation of Section III, exhibits the features typical of the slow reaction characteristic of the temperature range 500 - 800°K. Within a very short time $[HO_2]$ rises to a steady concentration of about 10^{10} molecules/cm^3. The log $[H_2O]$ and the log $[H_2O_2]$ increase steadily and slowly as nearly linear functions of log (time). The more reactive H, O and OH radicals are present in almost negligible amounts. Besides the concentrations, the sensitivity results for this entire pressure-temperature regime share many similar characteristics; their magnitudes strongly suggest certain mechanistic details. Reactions 11 through 14, which have already been recognized as important in an earlier study,[64] exhibit the largest sensitivities. In general, the chain is initiated by reaction 35, propagated by reaction 11, and then rapidly quenched by reaction 12. Reaction 40 restores the chain and reactions 13,

14, etc., promote eventual reaction. Obviously, HO_2 and H_2O_2 are important species in this regime and rate constants for reactions involving them should be more carefully determined. When the five wall reactions are included, the sensitivities to reactions 58 and 59 are very large. With minor exceptions, the rate constants for the fifteen reactions of the Baldwin, et al.,[27] set exhibit the largest sensitivities. This result is reassuring to kineticists who have devoted much time and effort to understanding the most critical elementary steps and also encouraging since these results demonstrate the power of sensitivity analysis in elucidating mechanistic details. The differences between the Baldwin mechanism and that indicated by the sensitivities (see Table III) are very slight. The chain-initiating reactions $H_2 + O_2 \longrightarrow 2OH$ and $H_2 + O_2 \longrightarrow H + HO_2$ as well as the reaction $O + H_2O_2 \longrightarrow H_2O + O_2$ appear to be more important than the reactions $H + HO_2 \longrightarrow 2OH$, $H + HO_2 \longrightarrow H_2O + O$, and $O + H_2O_2 \longrightarrow OH + HO_2$ of the Baldwin model. Furthermore, when the kinetic calculation was rerun with only the fifteen reactions of Table III, virtually no changes in kinetic behavior were observed. The concentration profiles for this run are shown in Figure 6.

More dramatic effects due to temperature are illustrated in Figures 7a, b and c, which correspond to kinetic runs carried out at $825°K$, $840°K$ and $875°K$ respectively. Figure 7a resembles Figures 3 and 5 at least qualitatively. Noticeable differences are a several hundredfold increase in overall reaction rate and substantial increases in the concentrations of the more reactive radical species, particularly H. The branching ratio $R_B = k_{11}/k_{12} M$ was about 0.3. The concentrations and sensitivity profiles are similar to those for the $700°K$ case; however, the normalized sensitivities to reactions 11

and 12 are nearly equally large in magnitude but opposite in sign. At
840°K (see Figure 7b) a slightly delayed explosion occurs. Before 0.40
seconds the kinetic behavior is similar to that at lower temperatures, yet
around 0.42 seconds extremely rapid concentration changes occur. The output
from the kinetic run indicates the concentrations of H, O, OH and H_2O to
increase by about two orders of magnitude within 10^{-3} sec. At short times
normalized sensitivities for reaction 11 and 12 are very large. At the
explosion time of 0.420 seconds, all normalized sensitivities are huge, many
larger than a million. A small variation in virtually any rate constant
changes the explosion time (but not the explosive behavior) for this process.
The largest sensitivities are for the rate constants for reactions 2, 3, 4,
5, 8, 9, 10, 11, 12, 20, 23 and 26. A chain-branching explosion is indicated
at this temperature and pressure, which seems to be close to the point where
the second and third limit pressures coalesce. At 875°K (see Figure 7c) the
explosion occurs almost immediately. The branching ratio is $R_B \approx 0.6$, and
$[HO_2]$ and $[H_2O_2]$ never get very large. Sensitivities are not nearly as
large as those for the 840°K case, but at 10^{-3} seconds the sensitivities of
$[H_2O]$ to the following rate constants are largest:

$$11(-10.4) > 12(7.3) > 35(-0.40) > 5(-0.28) \sim 20(-0.28)$$

$$> 1(-0.22) > 26(0.22) > 24(-0.16) > 3(-0.14) > 2(0.11)$$

The mechanism suggested by the sensitivity analysis was quite similar to that
suggested by screening analysis. This was often the case for many of the
calculations described in this paper. The mechanism suggested by the

sensitivities for this regime, however, differs considerably from that of Baldwin, et al., for the slow reaction. Since little attention seems to have been given in the literature to the mechanism for the explosive reaction regime, we have developed the mechanism given in Table IV. Note especially the importance of the H radical. The reaction at 320 torr for temperatures greater than 875°K exhibits similar explosive characteristics. Additionally, the overall reaction rate increases and normalized sensitivities generally decrease slowly as the temperature increases.

Several calculations were performed at 750°K to probe how the reaction proceeds for various initial pressures of the reactants in the neighborhood of the second explosion limit. For 750°K the calculations predict an explosion limit pressure of 80 ± 10 torr for a stoichiometric ratio of the reactants. This is in excellent agreement with results from several experiments, considering the effects of different vessel coatings used.[17,21,27,71] The mechanism for the fast reaction below this limit pressure suggested by the analysis of sensitivities is exactly that given in Table IV. Above the limit, the mechanism for the slow reaction is that of Table III, as one might reasonably expect. Perhaps more striking is that fact that a general _decrease_ in overall reaction rate is observed as the second explosion limit pressure is approached from the high pressure side; that is, the reaction is much slower at 100 torr than at several atmospheres. This is in semi-quantitative agreement with the experiments and calculations of Lewis and Von Elbe.[21] A partial explanation is the dominance of reaction 12 suggested by its large sensitivities in this regime. The effect of the concentration of M in the flux term, $k_{12}[M][H][O_2]$, is significant. Although just before the limit,

the reaction is very slow, at reactant pressures below 80 torr, the overall reaction rate increases several orders of magnitude. Large sensitivities to the $H + O_2 \longrightarrow OH + O$ step are observed and the branching ratio $R_B \gtrsim 0.5$. An "avalanche" of reactive radicals promotes rapid reaction.

The total pressure seems to play as significant a role as the initial partial pressures of H_2 and O_2. Addition of 50 - 100 torr of argon or nitrogen inhibits the explosion, lowering the limit pressure to below 30 torr at $750°K$ for the sum of the reactant pressures. This, too, is in agreement with an experiment.[71] The increased concentration of M makes the contribution to reaction 12 more dominant. This serves to slow down the reaction considerably just above the limit, but eventually, as higher pressures are reached, the presence of argon and/or nitrogen speeds up the reaction mildly. Several third body reactions, especially reactions 12 and 40, are important in the formation of H_2O via the $HO_2 \longrightarrow H_2O_2 \longrightarrow H_2O$ pathway.

Several other miscellaneous effects on the kinetic behavior in this regime are also considered. The calculations indicate that the explosion limit pressure increases steadily with temperatures from about 14 torr at $730°K$, where the first and second limits coalesce, to 320 torr at $840°K$, where the second and third limits meet. With regard to deviations from stoichiometric ratios of reactants, a mild increase in the second limit pressure is observed for an increase in the amount of hydrogen in the mixture. Analysis of initial concentration sensitivities indicates that most of the species are slightly more sensitive to the initial concentration of H_2 than to that of O_2. This is difficult to explain, although the dominance of reaction 12, $H + O_2 + M \longrightarrow HO_2 + M$, in this regime certainly plays a

role. Perhaps O_2 is less important, since it is present in a large, essentially constant concentration, whereas H is critical, because of reaction 12, and requires H_2 for formation. The effects of temperature and stoichiometry are in agreement with experimental results.[17, 21,72,73]

C. The third explosion limit.

The region in the vicinity of the third explosion limit has been particularly difficult to study in experiments.[17, 21,22] As we discussed in Section II, both chain and thermal mechanisms seem to play a role. We have carried out two types of calculations to probe this regime; one type assumes isothermal behavior, the other assumes adiabatic behavior. It is likely that the actual physical situation is somewhere between these two extremes. Heat and mass transport undoubtedly play a role as well.

In the previous subsection, we observed that an increase in pressure corresponds to an increase in overall reaction rate in between the second and third limits. The isothermal calculations indicate that this behavior persists up to at least one hundred atmospheres, and still no chain branching explosion is indicated. Moreover, no sharp limit seems to exist to define the third limit. Although the reaction proceeds very rapidly, concentration profiles are never spiked, but remain smooth and well-behaved. The sensitivities indicate that reactions 12, 13, 14 and 40 - the same as of those at much lower pressures - exhibit large sensitivities for most species. The concentrations of HO_2 and H_2O_2 are orders of magnitude higher than those of H, O and OH.

The adiabatic calculations are probably more useful in this regime. For these calculations a differential equation for the temperature is developed. (See the Appendix for a detailed derivation.) Numerical difficulties were encountered in solving the combined set of coupled equations [Eqs.(3.1) and (A.6)]. The temperature changes very rapidly, which in turn can cause even more rapid changes in the rate constants according to Eq.(2.1). Other numerical modelers have had trouble with this type of calculation.[74] To remedy this situation, we generally solved a difference equation for T similar to Eq.(A.6) at each step taken by the differential equation solver in treating the usual set of Eqs.(3.1). This method does not always reproduce the adiabatic flame temperature ($\sim 5800^\circ$K), which is defined as the highest temperature reached assuming that all the internal energy is used to raise the temperature of the reaction products. In the few cases where we solved the differential equations [Eqs.(3.1) and (A.6)] without numerical difficulty, the results obtained agreed with those obtained by the difference equation method. The difference equation method should give an accurate temperature and concentration profile for at least the initial 1500°K rise in temperature.

The adiabatic calculations that have been carried out in between the second and third explosion limits share certain characteristics in common. First of all, the adiabatic calculations all indicate about an order of magnitude increase in overall reaction rate in comparison to the isothermal calculations at the same initial conditions. In each run there is an induction period which may be very long in the case of the reaction just above the second limit pressure ($\sim 10^4$ sec) or very short at high pressures

and temperatures (≤ 0.5 sec). After this induction period, in which the temperature rises typically a few hundred degrees, there is a period of explosive reaction accompanied by a sharp temperature rise of a few thousand degrees. At these temperatures the nascent H_2O quickly reacts to form H, O and OH radicals, which are relatively more stable thermodynamically.

Both sensitivity analysis and screening analysis were used to elucidate mechanistic details. We investigated sensitivities to $\{A_i\}$, which is temperature-independent, rather than $\{k_i\}$. The analysis of sensitivities and fluxes indicates that, in the induction period, the usual mechanism for the reaction between the second and third limits given in Section IV.B is most appropriate. On the other hand, careful analysis suggests a different mechanism for the second stage of rapid reaction and sharp temperature rise. Radical concentrations of H and O increase considerably in this regime indicating the importance of several chain reactions, most notably 10, 11, 20, 22, 24, 25, 26 and 31. At such high temperatures reactions with large activation energies like 5, 18, 19, 36 and 39 also exhibit reasonably large sensitivities. It is clear that many elementary reaction steps contribute in the vicinity of the third explosion limit, as the usual slow mechanism is supplanted by a chain mechanism including even some endothermic reactions.

On the basis of these calculations a few conclusions can be reached regarding the thermal regime studied here. First there does not seem to be any clear-cut, sharp third limit pressure-temperature boundary, as for the first and second limits. The calculations do indicate that at high pressures and high temperatures, there are short induction periods and very large reaction rates. At lower pressures and temperatures, induction periods are

long and initial overall reaction rates are small. These results are in qualitative agreement with the experimental result described in Section II. According to several theories,[16,21] the length of the induction period and the initial reaction rate - which $\underline{can}$ be determined for various pressures and temperatures from calculations - are key indicators of whether an explosion will or will not occur. The results of this study lend credence to the idea that at low temperatures and pressures induction periods are so long that the heat may be transported to the walls of the reaction vessel and dissipated before reaction occurs. At higher pressures and temperatures reaction occurs before the heat can be dissipated.

As an epilogue to this section we present, in Table V, a list of the reactions from the reaction set of Table I which seem to play a minor, if any, role in the kinetics of the process regardless of the temperature-pressure regime considered. This information was obtained from a careful analysis of sensitivities. Reruns of a few calculations indicated them to be of very little significance. Brief explanations for their unimportant stature are also suggested.

V. Sensitivity Analysis of an Experiment to Determine the Rate Constant for $H + O_2 + M \longrightarrow HO_2 + M$

We describe here the analysis of a shock tube experiment carried out at temperatures in the range 980 - 1176°K by Slack.[40] In this study experimentally determined induction times were matched with numerically predicted induction times to obtain a rate constant for the important reaction 12 in Table I. A model containing sixteen reaction steps was used for the numerical predictions. Slack investigated how variations in the numerical values of rate constants in the model affected the rate constant for $H + O_2 + M \longrightarrow HO_2 + M$ (brute force approach). Our motivation for studying this experiment was to demonstrate the power and utility of derived sensitivities for a particularly suitable experimental/theoretical study relevant to the H_2-O_2 system. The derived sensitivities, which have already been considered in an earlier paper,[14] were compared with Slack's results.

To simulate one of the shock tube experiments, we have carried out two isothermal calculations at 993°K. The initial pressure of the reactants, which are present in a stoichiometric ratio, is 64 torr. Nitrogen (64 torr) was used as a diluent. Three calculations were carried out: the first used the usual 57 reactions of Table I, the second included only those sixteen reactions in Slack's model with his rate constant parameters, and the third included those reactions but used the rate constant parameters of Table I for them. No appreciable differences are detectable for the three runs. The calculated concentration profiles for the first run are shown in Figure 8. The calculated induction time is 5×10^{-4} sec, in excellent agreement with the experimental result, which, according to the oscilloscope

trace given in reference 40, is at most 10% higher. Furthermore the net conversion rates (i.e., flux contributions) are in semi-quantitative agreement with those given by Slack.

The derived sensitivities that are suitable for analyzing this experiment are of the form $\left(\dfrac{\partial k_{12}}{\partial k_j}\right)_{\widetilde{\underline{k}},[H_2O]}$ $\left[\text{or } \left(\dfrac{\partial k_{12}}{\partial [H_2O]}\right)_{\widetilde{\underline{k}}}\right]$. The notation[14] $\widetilde{\underline{k}}$ refers to all the rate constants except k_j (or $[H_2O]$) and k_{12}. k_{12} is determined in this experiment; thus it is indeed appropriate to consider it an output quantity. $[H_2O]$ is properly considered as an input parameter, since its emission spectrum is monitored in the experiment. The relevant dimensionless derived sensitivity coefficients $\left(\dfrac{\partial \ln k_{12}}{\partial \ln k_j}\right)_{\widetilde{\underline{k}},[H_2O]}$ $\left[\text{or } \left(\dfrac{\partial \ln k_{12}}{\partial \ln [H_2O]}\right)_{\widetilde{\underline{k}}}\right]$ have been calculated and rank-ordered. The results at 4×10^{-4} are:

$$11(26) > 26(7.5) > 20(4.5) > [H_2O](2.4) > 35(2.4) > 2(-8.1 \times 10^{-2})$$

$$> 24(-4.0 \times 10^{-2}) > 34(2.4 \times 10^{-2}) > 4(1.5 \times 10^{-2})$$

$$\gtrsim 3(1.5 \times 10^{-2}) > 43(-1.2 \times 10^{-2}) > 16(-3.6 \times 10^{-3})$$

The large sensitivity of k_{12} to k_{11} is expected. The experiment is carried out in high temperature regime, where reaction 11 dominates. The brute force sensitivities suggest the rate constants for the following reactions to be important in determining k_{12}: 4, 11, 13, 14, 20, 26 and 40. Not all of the results of reference 40 agree with ours. Reactions 13, 14 and 40 - important in the slow regime between the second and third explosion limits - are not nearly so critical for the rapid reaction characteristic of this pressure-temperature regime. On the other hand, the chain-initiating reaction, 35, is

more important than the brute force results indicate. A possible reason for the discrepancies observed is that brute force sensitivity analysis is somewhat difficult to implement systematically even for small models. Clearly, to determine k_{12} by matching experimentally determined and numerically predicted induction times, it is imperative to have the most accurate rate constant parameters available for reactions 11, 20, 26 and 35, since even slight errors can introduce large uncertainties in k_{12} because of the high correlations.

VI. Study of a Related Reaction: The Decomposition of Hydrogen Peroxide

To demonstrate the versatility of the reaction set presented in Table I, we present results of a few calculations performed to study the decomposition of hydrogen peroxide, a process which exhibits many similarities to the slow reaction of hydrogen and oxygen between the second and third limits. The net reaction is

$$H_2O_2(g) \longrightarrow H_2O(g) + \tfrac{1}{2}O_2(g)$$

Besides this process, other less-studied reactions (e.g., $2HO_2 \longrightarrow H_2O_2 + O_2$) involved in the H_2-O_2 system could benefit from the type of analysis presented in this paper.

Two isothermal calculations were carried out at a temperature of $750°K$. Partial pressures of H_2O_2 and argon were 213 torr and 360 torr, respectively. For the first calculation the usual 57 reaction set from Table I was utilized. The resulting concentration profiles are given in Figure 9. A slow, steady reaction possessing many features of the regime between the second and third limits for hydrogen combustion is indicated. As in the usual slow reaction, $[HO_2]$ rapidly reaches a steady concentration and remains relatively constant for several seconds. A previous study[75] assumed $[HO_2] \sim 0.01[H_2O_2]$; this apparently is only true after several hundred seconds. Virtually no chain-branching is indicated: $R_B \lesssim 0.1$, and H and O are present in negligible amounts. Normalized sensitivities were computed for several times and all species concentrations for this reaction. The rank-ordered normalized sensitivities at twenty seconds for $[OH]$ are:

$$40(1.0) \gtrsim 28(-1.0) > 13(-1.8 \times 10^{-3}) > 16(-2.3 \times 10^{-4})$$

Most of the other rate constants exhibit sensitivities that are much smaller. When a second calculation was carried out including only the four reactions shown above as the model, the overall rate of reaction was within 10% of the previously mentioned calculations, although some intermediate species concentrations are not as accurately reproduced. Several other reactions are of some importance, most notably, 6, 7, 17, 18, 26 and 37. Note that the mechanism suggested by analysis of the sensitivities corresponds roughly to that of the usual slow reaction between H_2 and O_2.

Overall the agreement with relevant experimental results and earlier theoretical models is reasonably good. Several experiments have already established the nonchain character of this reaction.[76] Meyer, et al.,[77] have studied this process at somewhat higher temperatures, and it is interesting that their suggested mechanism consists of the reactions

$$H_2O_2 + M \longrightarrow 2OH + M$$

$$OH + H_2O_2 \longrightarrow HO_2 + H_2O$$

$$2HO_2 \longrightarrow H_2O_2 + O_2$$

and possibly

$$OH + HO_2 \longrightarrow H_2O + O_2 .$$
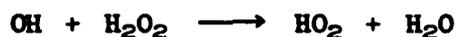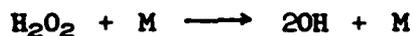
This is exactly the mechanism suggested by the sensitivities. Meyer, et al., applied the steady state approximation[78] to [OH] and [HO_2] in the first

three reactions above to obtain the result

$$\frac{d[H_2O_2]}{dt} = -\chi[M][H_2O_2] \qquad (6.1)$$

where $\chi = 2k_{40}$. We find this to be an adequate representation on the basis of the results presented here, with the exception that χ is approximately $1.5k_{40}$ rather than $2k_{40}$.

VII. Discussion and Conclusions

To the best of our knowledge, this work represents the most comprehensive modeling study available for the H_2-O_2 system, which has been carefully studied experimentally and theoretically for many years. In many cases the modeling results could be anticipated by experimental results and scientific intuition, yet these calculations still serve an important function by amplifying and clarifying certain important features of this system.

An important contribution is Table I, which lists a useful reaction set and appropriate rate constant parameters. Although an excellent compilation has already been provided by Baulch, et al.,[29] for this system, the present evaluations are useful since many of these rate constant parameters have been revised and updated since 1971 and have not yet been assembled into a single source.[79] Also, the fact that modeling results for this reaction set agree so well with experiment, attests to its validity.

A second important facet of this work is the extensive use of sensitivity analysis. The results of this work demonstrate the power and utility of a proper analysis of sensitivity information. Sensitivity analysis was chiefly applied in this study to probe mechanistic behavior. Although it is true that most of the mechanistic details could be inferred from experimental evidence by careful analysis, determination of rate constant sensitivities by a simple calculation can reduce the amount of work considerably. It is difficult to determine which rate constants are important by studying of a list of possible reactions. (The mere magnitude of the rate constants is often a misleading indicator.) Sensitivity aids in this determination, so that more complicated analysis may not be warranted. The mechanisms suggested by the

sensitivities given in Tables III and IV should be particularly useful for additional model studies. Moreover, Section VI demonstrates the use of derived sensitivities in interpreting and analyzing the results of kinetics experiments for determining rate constants. By establishing the correlations of the desired rate constant to other rate constants in the system, one may obtain more realistic error bounds for the experimental determination. Kinetics experiments could conceivably be designed to minimize correlations with the desired rate constants.

The methodology and results presented in this paper should be useful for additional studies of this model as well as for other combustion systems. The methodology can certainly be extended to any model one wishes to study. An algorithm for numerical modeling and sensitivity analysis has been constructed and extensively tested and is easy to implement for isothermal mass action kinetic calculations.[14,80] Besides the methodology, the H_2-O_2 kinetic results from the present or similar studies should be useful to the experimental kineticist in determining which elementary steps to concentrate his efforts on. We found that many reactions involving HO_2, particularly reaction 12, are important in the regime between the second and third explosion limits. These reactions have been extensively studied,[81,82] yet clearly some additional work is called for. The uncertainty estimates given in Table I could be combined with the sensitivity results to assign each reaction a sensitivity-uncertainty index as a guideline for useful experiments.[83] The H_2-O_2 kinetic results may be useful in combustion studies of other systems. Westbrook, et al.,[84] have found that the branching ratio of $H + O_2 \longrightarrow OH + O$ and $H + O_2 + M \longrightarrow HO_2 + M$ is critical in

determining the length of the induction period for a numerical model of methane combustion. The important elementary steps in the H_2-O_2 system may very well be the ones that are critical in more complicated systems.

We conclude this work with a few suggestions for future work suggested by our results on this and similar combustion systems. It certainly would be useful to study more carefully the nature of explosions characteristic of many combustion systems. Obviously explosions result from some sort of instability. For the H_2-O_2 system this instability is evident in the calculated concentration profiles (Figure 7) and in the sensitivity behavior in the neighborhood of the explosion limits. Thus catastrophe theory[85] or stability theory,[86-88] which has already been applied to the H_2-O_2 system,[89] might be useful approaches to this problem, possibly in conjunction with sensitivity analysis. The results of the present work could be used to provide the most salient features of the explosive system.

Aside from general studies of explosive phenomena, the results of this work suggest that additional studies of the first and third limits of the H_2-O_2 system would be useful. Mass diffusion should properly be included into the model for studies of the first limit, and heat transport is clearly important for studying the third limit. A sensitivity analysis of the resulting partial differential equations involved in such studies is somewhat involved, but work is progressing in this area and should prove to be important.[90] The results of the present study - concentrations, sensitivity profiles, and the reaction sets of Tables III and IV - should be useful guides for treating these two limits as well as other pressure-temperature regimes.

Appendix

Derivation of the Expression for $\dfrac{dT}{dt}$ in Adiabatic Modeling Calculations

The first law of thermodynamics (including the effects of chemical reactions) is given by

$$dU = dq + dw + \sum_{i=1}^{n} \left(\frac{\partial U}{\partial s_i}\right) ds_i \qquad (A.1)$$

where U denotes the internal energy of the system, dq refers to the differential change in the heat added to the system, dw is the differential work done on the system $\left(-\int P_{ext} \, dV\right)$, and s_i refers to the number of moles of species i. Since adiabatic conditions are assumed and since the reaction vessel is of constant volume, dq = dw = 0. Moreover, dU = dH - d(PV) = dH - V dP, so that Eq.(A.1) becomes

$$dU = \sum \left(\frac{\partial H}{\partial s_i}\right) ds_i - V \sum \left(\frac{\partial P}{\partial s_i}\right) ds_i \qquad (A.2)$$

Dividing through by V and noting that $dU = \sum s_i C_{v_i} dT$ we obtain

$$\sum_i y_i C_{v_i} dT = \sum \left(\frac{\partial H}{\partial s_i}\right) dy_i - \sum \left(\frac{\partial P}{\partial y_i}\right) dy_i \qquad (A.3)$$

where $y_i = s_i/V$ is the usual i-th species concentration and C_{v_i} is the i-th specific heat capacity at constant volume. Since the ideal gas law is assumed to be valid for all species, we obtain

$$\sum y_i C_{v_i} \, dT = \sum \left[h_i - RT \right] dy_i \qquad (A.4)$$

where $h_i \equiv \dfrac{\partial H}{\partial s_i}$ is the specific enthalpy for the i-th species. Now we formally differentiate with respect to time to obtain

$$\frac{dT}{dt} = \frac{\sum \left[h_i - RT \right] \dfrac{dy_i}{dt}}{\sum C_{v_i} y_i} \qquad (A.5)$$

Since h_i and C_{v_i} are assumed to be linear functions of temperature $\left(h_i = h_i^{(o)} + h_i^{(1)} T \quad \text{and} \quad C_{v_i} = C_{v_i}^{(o)} + C_{v_i}^{(1)} T \right)$ we obtain

$$\frac{dT}{dt} = \frac{\sum \left[h_i^{(o)} + \left(h_i^{(1)} - R \right) T \right] \dfrac{dy_i}{dt}}{\sum \left[C_{v_i}^{(o)} + C_{v_i}^{(1)} T \right] y_i} \qquad (A.6)$$

Note that Eq.(A.6) is coupled to the usual set of equations for the species concentrations, Eqs.(3.1).

References

1. J. Phys. Chem. $\underline{81}$, #25 (1977). This issue contains many articles on applications of numerical models in chemical kinetics.

2. A. Charnes and W. W. Cooper, _Management Models and Industrial Applications of Linear Programming_ (Wiley, New York, 1961).

3. D. H. Meadows, _et al._, _The Limits to Growth_ (Potomac Associates/Universe Books, New York, 1972).

4. C. A. S. Hall and J. W. Day, Jr., _Ecosystem Modeling in Theory and Practice_ (Wiley, New York, 1977).

5. D. R. Hardesty, in _Combustion Measurements: Modern Techniques and Instrumentation_, R. Goulard, ed. (Academic, New York, 1976).

6. See, e.g., D. L. Allara and D. Edelson, Int. J. Chem. Kinet. $\underline{7}$, 479 (1975).

7. One exception is a study of the sensitivities of a model for methane combustion described in A. A. Boni and R. C. Penner, Combust. Sci. Technol. $\underline{15}$, 99 (1976).

8. R. P. Dickinson and R. J. Gelinas, J. Comp. Phys. $\underline{21}$, 123 (1976).

9. R. W. Atherton, R. B. Schainker and E. R. Ducot, AIChE J. $\underline{21}$, 441 (1975).

10. Y. Bard, _Nonlinear Parameter Estimation_ (Academic, New York, 1974).

11. R. I. Cukier, C. M. Fortuin, K. E. Shuler, A. G. Petschek and J. H. Schaibly, J. Chem. Phys. $\underline{59}$, 3873 (1973).

12. R. I. Cukier, H. B. Levine and K. E. Shuler, J. Comp. Phys. 26, 1 (1978).

13. J.-T. Hwang, E. P. Dougherty, S. Rabitz and H. Rabitz, J. Chem. Phys. 69, 5180 (1978).

14. E. P. Dougherty, J.-T. Hwang and H. Rabitz, J. Chem. Phys. 71, 1794 (1979).

15. J.-T. Hwang and H. Rabitz, J. Chem. Phys. 70, 4609 (1979).

16. I. Glassman, Combustion (Academic, New York, 1977).

17. G. Dixon-Lewis and D. J. Williams, in Comprehensive Chemical Kinetics, C. H. Bamford and C. F. H. Tipper, eds., Vol. 17, (Elsevier, Amsterdam, 1977), pp. 1-248.

18. C. N. Hinshelwood and A. T. Williamson, The Reaction Between Hydrogen and Oxygen (Oxford University Press, Oxford, 1934).

19. N. Semenov, Chemical Kinetics and Chain Reactions (Oxford University Press, 1935).

20. W. Jost, Explosion and Combustion Processes in Gases (McGraw Hill, New York, 1946).

21. B. Lewis and G. von Elbe, Combustion, Flames and Explosions of Gases (Academic, New York, 1961).

22. G. J. Minkoff and C. F. H. Tipper, Chemistry of Combustion Reactions (Butterworths, London, 1962).

23. A. A. Frost and N. H. Alyea, J. Am. Chem. Soc. 55, 3227 (1933); 56, 1251 (1934).

24. W. J. Moore, Physical Chemistry (Prentice-Hall, Englewood Cliffs, N.J., 1972).

25. R. N. Pease, J. Am. Chem. Soc. 52, 5106 (1930); 53, 3188 (1931).

26. J. A. Miller and R. J. Kee, J. Phys. Chem. 81, 2534 (1977).

27. R. R. Baldwin, M. E. Fuller, J. S. Hillman, D. Jackson, and R. W. Walker, J. C. S. Faraday Trans. I 4, 635 (1974).

28. R. J. Gelinas, Methane Combustion Kinetics: Final Report, SAI/PL-NI-77-02, Prepared for the Naval Research Laboratory, Washington, D.C., October 1977.

29. D. L. Baulch, D. D. Drysdale, D. G. Horne and A. C. Lloyd, Evaluated Kinetic Data for High Temperature Reactions, Vol. 1, (Butterworths, London, 1972).

30. P. Walkauskas and F. Kaufman, 15-th Int. Symp. Combust. (Combustion Institute, Pittsburgh, Pa., 1975), p. 691.

31. J. E. Bennett and D. R. Blackmore, Proc. Roy. Soc. A305, 553 (1968).

32. A. C. Lloyd, Int. J. Chem. Kinet. 6, 169 (1974).

33. A. A. Westenberg and N. de Haas, J. Chem. Phys. 58, 4061 (1973).

34. V. S. Engleman, Survey and Evaluation of Kinetic Data on Reactions in Methane/Air Combustion, EPA-660/2-76-003, Prepared for the EPA, January, 1976.

35. R. P. Overend, G. Paraskevopoulos and R. J. Cvetanović, Can. J. Chem. 55, 1598 (1977).

36. R. B. Klemm, W. A. Payne and L. J. Stief, Proc. Symp. Chem. Kinet. Data for the Upper and Lower Atmosphere, Int. J. Chem. Kinet. 7, Supp. 1, 61 (1975).

37. K. Schofield, J. Phys. Chem. Ref. Data 2, 25 (1973).

38. G. B. Skinner, A. Lifshitz, K. Scheller and A. Burcat, J. Chem. Phys. 56, 3853 (1972).

39. K. H. Eberius, K. Hoyermann and H. Gg. Wagner, 13th Int. Symp. Combust., (Combustion Institute, Pittsburgh, Pa., 1971), p. 713.

40. M. W. Slack, Comb. Flame 28, 241 (1977).

41. R. F. Hampson, Jr., and D. Garvin, NBS Technical Note #866, NBS, Washington, D.C., June 1975.

42. V. N. Kondratiev, Dokl. Akad. Nauk SSSR 137, 120 (1961); English translation, p. 235.

43. G. S. Bahn, Reaction Rate Compilation for the H-O-N System, (Gordon and Breach, New York, 1968); attributed to private communication with W. Chinitz.

44. G. S. Bahn, Pyrodynamics 2, 315 (1965).

45. I. M. Campbell and B. A. Thrush, Trans. Faraday Soc. 64, 1265 (1968).

46. A. F. Sirifim, G. C. Williams, N. Lambert and A. Padia, Proc. 2-nd Conf. on Natural Gas Res. and Technol., Atlanta, June 1972.

47. E. A. Albers, K. Hoyermann, H. Gg. Wagner and J. Wolfrum, 13-th Int. Symp. Combust., (Combustion Institute, Pittsburgh, Pa., 1971), p. 81.

48. D. D. Davis, Can. J. Chem. 52, 1405 (1974).

49. Climatic Impact Assessment Program, I. The Natural Stratosphere, CIAP Office, Dept. of Transportation, Washington, D.C., 1975.

50. H. L. Petersen and C. B. Kretschmer, Aerojet-General Corporation Report TN-38, AD 283 044, November 1960.

51. W. E. Wilson, Jr., J. Phys. Chem. Ref. Data 1, 535 (1972).

52. I. W. M. Smith and R. Zellner, J. C. S. Faraday Trans. II 70, 1045 (1974).

53. F. Stuhl and H. Niki, J. Chem. Phys. 57, 3671 (1972).

54. C. J. Jachimowski and W. M. Houghton, Comb. Flame 17, 25 (1971).

55. R. W. Walker in Reaction Kinetics: A Specialist Periodical Report, Vol. 1, (Billing and Sons, London, 1975), pp. 161 ff.

56. D. R. Stull and H. Prophet, JANAF Thermochemical Tables, 2-nd ed., NBS publication, NSRDS-NBS 37, 1971.

57. J. B. Homer and I. R. Harle, Proc. Roy. Soc. A314, 585 (1970).

58. D. L. Baulch, D. D. Drysdale, J. Duxbury and S. J. Grant, _Evaluated Kinetic Data for High Temperature Reactions_, Vol. 3, (Butterworths, London, 1976).

59. D. B. Olson and W. C. Gardiner, Proc. ACS Meeting, New Orleans, La., 1977.

60. D. E. Jensen and G. A. Jones, Comb. Flame 22, 1 (1978).

61. H. S. Johnston, _Gas Phase Reaction Kinetics of Neutral Oxygen Species_, NBS-NSRDS 20, NBS, Washington, D.C., 1968.

62. R. Shaw, Int. J. Chem. Kinet. 9, 929 (1977).

63. R. Simonaitis and J. Heicklen, J. Phys. Chem. 77, 1096, 1932 (1973).

64. D. E. Hoare, G. B. Peacock and G. R. D. Ruxton, Trans. Faraday Soc. 63, 2498 (1967).

65. I. K. Shaklazaryan, G. A. Sachyan, A. G. Philipossyan and A. B. Malbandyan, Int. J. Chem. Kinet. 6, 693 (1974).

66. JANAF Interim Thermochemical Tables, (Dow Chemical Company, Midland, Michigan, December 1960).

67. A. A. Frost and R. G. Pearson, _Kinetics and Mechanism_ (New York, Wiley, 1961).

68. A. C. Hindmarsh, _Gear: Ordinary Differential Equations System Solver_, UCID-30001, Rev. 3, Lawrence Livermore Laboratory, Livermore, Ca., December 1974; (b) C. W. Gear, ACM Comm. 14, 176 (1971).

69. R. I. Cukier, H. B. Levine and K. Shuler, J. Phys. Chem. 81, 2365 (1977).

70. R. N. Pease, in Combustion Processes, ed. B. Lewis, R. N. Pease and H. S. Taylor, (Princeton University Press, Princeton, N.J., 1956).

71. A. C. Howson and R. F. Simmons, 11-th Int. Symp. Combust., (Combustion Institute, Pittsburgh, Pa., 1966), p. 1081.

72. D. R. Warren, Proc. Roy. Soc. A211, 86, 96 (1952).

73. B. Lewis and G. von Elbe, J. Chem. Phys. 9, 194 (1941); 10, 366 (1951).

74. D. Indritz, private communication.

75. A. Tessier and W. Forst, Can. J. Chem. 52, 794 (1974).

76. R. R. Baldwin and D. Brattan, 8-th Int. Symp. Combust., (Williams and Wilkins, 1962), p. 110.

77. E. Meyer, H. A. Olschewski, J. Troe and H. Gg. Wagner, 14-th Int. Symp. Combust., (Combustion Institute, Pittsburgh, Pa., 1968), p. 345.

78. S. W. Benson, The Foundations of Chemical Kinetics, (McGraw Hill, New York, 1960).

79. This situation should change in the near future. N. Cohen, et al., plan to publish an updated evaluation of rate constants for the H_2-O_2 system in 1980, private communication.

80. E. P. Dougherty and H. Rabitz, Int. J. Chem. Kinet., to be published, 1979.

81. Reaction Kinetics: A Specialist Periodical Report, Vol. 1, (Billing and Sons, London, 1975), Ch. 4.

82. Reaction Kinetics: A Specialist Periodical Report, Vol. 2, (Billing and Sons, London, 1977), especially pp. 296-330.

83. M. C. Dodge and T. A. Hecht, Proc. Symp. Chem. Kinet. Data for the Upper and Lower Atmosphere, Int. J. Chem. Kinet. 7, Supp. 1, 155 (1975).

84. C. K. Westbrook, I. Creighton, C. Lund and F. L. Dryer, J. Phys. Chem. 81, 2542 (1977).

85. R. Thom, Structural Stability and Morphogenesis (Benjamin-Cummings, New York, 1973).

86. W. Hurewicz, Lectures on Ordinary Differential Equations (Wiley, New York, 1958).

87. H. T. Davis, Introduction to Nonlinear Differential and Integral Equations, (Dover, New York, 1962).

88. B. F. Gray and C. H. Yang, J. Phys. Chem. 69, 2747 (1965).

89. C. H. Yang and B. F. Gray, 11-th Int. Symp. Combust. (Combustion Institute, Pittsburgh, Pa., 1967), p. 1099.

90. M. Demiralp and H. Rabitz, in progress; M. Koda, A. Dogru and J. Seinfeld, J. Comp. Phys. 30, 259 (1979).

Table I. Reaction Set for H_2-O_2 Calculations. $k_i = A_i T^{B_i} \exp(-C_i/T)$ [a]

Reaction Number	Reaction [b]	A_i	B_i	C_i	$\Delta \log_{10} k_i$ [c]	References [d]
1	$2H + M \longrightarrow H_2 + M$, M = Ar, N_2	9.0 (17)	-1.00		0.3	17, 29
2*e	$H + HO_2 \longrightarrow H_2 + O_2$	2.5 (13)		350	0.8	29, 30, 31
3*	$H + HO_2 \longrightarrow H_2O + O$	5.0 (13)		500	1.0	32, 33
4*	$H + HO_2 \longrightarrow 2 OH$	2.5 (14)		950	1.0	32
5	$H + H_2O \longrightarrow H_2 + OH$	1.4 (14)	-0.03	10,200	0.1	29, 34
6*	$H + H_2O_2 \longrightarrow H_2 + HO_2$	1.7 (12)		1,900	0.8	29
7*	$H + H_2O_2 \longrightarrow H_2O + OH$	5.0 (14)		5,000	0.4	29, 36
8	$H + O + M \longrightarrow OH + M$, M = Ar, N_2	7.9 (15)			1.2	37
9	$H + OH \longrightarrow H_2 + O$	8.3 (9)	1.00	3,500	0.2	29, 38
10	$H + OH + M \longrightarrow H_2O + M$, M = Ar	8.4 (21)	-2.00		1.5	29
10a	$H + OH + M \longrightarrow H_2O + M$, M = N_2	2.2 (22)	-2.00		1.5	29
11*	$H + O_2 \longrightarrow OH + O$	2.3 (14)		8,400	0.2	39
12*	$H + O_2 + M \longrightarrow HO_2 + M$, M = Ar	2.1 (18)	-1.00		0.4	40
12a	$H + O_2 + M \longrightarrow HO_2 + M$, M = N_2	3.0 (18)	-1.00		0.4	40
13*	$2 HO_2 \longrightarrow H_2O_2 + O_2$	1.8 (13)		500	1.0	41
14*	$H_2 + HO_2 \longrightarrow H_2O_2 + H$	6.0 (11)		9,300	0.6	29
15	$HO_2 + H_2O \longrightarrow H_2O_2 + OH$	1.8 (13)		15,100	0.4	42

Table I. (continued)

Reaction Number	Reaction	A_1	B_1	C_1	$\Delta \log_{10} k_1$	References
16	$OH + HO_2 \longrightarrow H_2O + O_2$	5.0 (13)		500	0.5	32
17	$OH + HO_2 \longrightarrow H_2O_2 + O$	5.2 (10)	0.50	10,600	2.0	43
18	$HO_2 + M \longrightarrow H + O_2 + M,\ M = Ar$	2.1 (15)		23,000	0.2	29
18a	$HO_2 + M \longrightarrow H + O_2 + M,\ M = N_2$	2.8 (15)		23,000	0.2	29
19	$HO_2 + M \longrightarrow O + OH + M,\ M = Ar, N_2$	6.8 (19)	-0.43	32,200	2.0	34, 44
20*	$H_2 + O \longrightarrow H + OH$	1.8 (10)	1.00	4,480	0.2	29, 45
21	$O + H_2O \longrightarrow H + HO_2$	4.8 (14)	0.45	28,700	2.0	32, 34
22	$O + H_2O \longrightarrow 2\, OH$	5.8 (13)		9,070	0.4	46, 47
23*	$O + H_2O_2 \longrightarrow OH + HO_2$	2.0 (13)		2,950	1.0	48, 49
24	$O + OH \longrightarrow H + O_2$	3.0 (12)	0.28		1.0	29, 34, 49
25	$O + OH + M \longrightarrow HO_2 + M,\ M = Ar, N_2$	8.0 (16)			2.0	34, 44, 50
26*	$H_2 + OH \longrightarrow H_2O + H$	2.5 (13)		2,600	0.1	29
27	$H_2O + OH \longrightarrow H_2O_2 + H$	2.4 (14)		40,500	1.2	29
28*	$OH + H_2O_2 \longrightarrow H_2O + HO_2$	1.0 (13)		910	0.3	29
29	$2\, OH \longrightarrow H + HO_2$	1.2 (13)		20,200	0.8	29
30	$2\, OH \longrightarrow H_2 + O_2$	1.7 (13)		24,100	0.8	54

Table I. (continued)

Reaction Number	Reaction	A_1	B_1	C_1	$\Delta \log_{10} k_1$	References
31	$2\,OH \longrightarrow H_2O + O$	6.3 (12)		550	0.4	29
32	$2\,OH + M \longrightarrow H_2O_2 + M$, $M = Ar$	2.7 (14)		$-2{,}650$	0.8	51
32a	$2\,OH + M \longrightarrow H_2O_2 + M$, $M = N_2$	8.4 (14)		$-2{,}650$	0.8	29, 51
33	$OH + M \longrightarrow O + H + M$, $M = Ar, N_2$	6.1 (15)		51,100	1.5	34, 37
34	$H_2 + O_2 \longrightarrow H + HO_2$	3.1 (13)		28,700	0.9	55
35	$H_2 + O_2 \longrightarrow 2\,OH$	1.7 (13)		24,200	1.2	54, 56
36	$H_2O + O_2 \longrightarrow OH + HO_2$	5.6 (13)	0.17	36,600	1.5	32, 34
37	$H_2O_2 + O_2 \longrightarrow 2\,HO_2$	3.0 (13)		21,600	1.0	29, 55
38	$H_2 + M \longrightarrow 2\,H + M$, $M = Ar, N_2$	2.2 (14)		48,300	0.8	17, 29
39	$H_2O + M \longrightarrow H + OH + M$, $M = Ar$	4.0 (23)	-2.20	59,000	0.6	29, 51, 57
39a	$H_2O + M \longrightarrow H + OH + M$, $M = N_2$	1.0 (24)	-2.20	59,000	0.6	29, 51, 57
40*	$H_2O_2 + M \longrightarrow 2\,OH + M$, $M = Ar$	6.0 (16)		22,900	0.3	29
40a	$H_2O_2 + M \longrightarrow 2\,OH + M$, $M = N_2$	1.2 (17)		22,900	0.3	29

Table I. (continued)

Reaction Number	Reaction	A_i	B_i	C_i	$\Delta \log_{10} k_i$	References
41	$2O + M \longrightarrow O_2 + M$, M = Ar	1.9 (13)		-900	0.6	58
41a	$2O + M \longrightarrow O_2 + M$, M = N$_2$	6.0 (13)		-900	0.6	58
42	$O_2 + M \longrightarrow 2O + M$, M = Ar	1.8 (18)	-1.00	59,400	0.6	58
42a	$O_2 + M \longrightarrow 2O + M$, M = N$_2$	5.4 (18)	-1.00	59,400	0.6	58
43	$O + HO_2 \longrightarrow O_2 + OH$	5.0 (13)		500	0.8	32
44	$O_2 + OH \longrightarrow HO_2 + O$	1.3 (13)	0.18	28,200	1.2	32, 34
45	$H_2 + HO_2 \longrightarrow H_2O + OH$	6.5 (11)		9,400	1.0	59, 60
46	$H_2O + OH \longrightarrow H_2 + HO_2$	7.2 (9)	0.43	36,100	1.4	34, 59, 60
47*	$O + H_2O_2 \longrightarrow H_2O + O_2$	8.4 (11)		2,130	1.0	41
48	$H_2O + O_2 \longrightarrow H_2O_2 + O$	3.4 (10)	0.52	44,800	1.4	42, 56
49	$O + O_2 + M \longrightarrow O_3 + M$, M = Ar	4.3 (12)		-1,050	0.6	61
49a	$O + O_2 + M \longrightarrow O_3 + M$, M = N$_2$	6.9 (12)		-1,050	0.6	29, 61
50	$O_3 + M \longrightarrow O + O_2 + M$, M = Ar	2.5 (14)		11,400	0.6	58
50a	$O_3 + M \longrightarrow O + O_2 + M$, M = N$_2$	4.0 (14)		11,400	0.6	58

Table I. (continued)

Reaction Number	Reaction	A_i	B_i	C_i	$\Delta \log_{10} k_i$	References
51	$O + O_3 \longrightarrow 2 O_2$	1.1 (13)		2,300	0.4	41
52	$2 O_2 \longrightarrow O + O_3$	1.2 (13)		50,500	0.6	41, 61
53	$H + O_3 \longrightarrow OH + O_2$	2.3 (11)	0.75		1.8	62
54	$OH + O_2 \longrightarrow H + O_3$	4.4 (7)	1.44	38,600	2.0	56, 62
55	$OH + O_3 \longrightarrow HO_2 + O_2$	9.6 (11)		1,000	0.6	41
56	$HO_2 + O_2 \longrightarrow OH + O_3$	9.0 (8)			2.0	27
57	$HO_2 + O_2 \longrightarrow OH + 2 O_2$	2.0 (10)		1,000	1.0	63
58^f	$HO_2 \longrightarrow$ wall	1.0 (-1)			--	64, 65
59	$H_2O_2 \longrightarrow$ wall	1.0 (-2)			--	64, 65
60	$H \longrightarrow$ wall	3.0 (0)			--	64, 65
61	$O \longrightarrow$ wall	1.7 (1)			--	64, 65
62	$OH \longrightarrow$ wall	1.7 (1)			--	64, 65

Table I. (continued)

[a] Temperature range: 300 - 2500°K. Units are in terms of moles, cm^3, sec and degrees K. Numbers in parentheses denote powers of ten. Missing entries are all zero.

[b] M denotes all other species present as third bodies. The numerical values for the third-order reactions here are for M = Argon or Nitrogen. We took numerical values for these rate constants for M = H, H_2, etc. to be 1.6 X those shown for the case where M = Argon. Reference 29 was used as a guide for assigning these third-body efficiencies.

[c] Only rough estimates of the rate constant uncertainties are given.

[d] In several cases the authors made slight modifications to the numerical values of the rate constant parameters given in the references. Often a compromise was reached. This explains the reason for two or three citations for a single elementary step.

[e] The reaction numbers marked with an asterisk (*) are those of the Baldwin, et al., reaction set of reference 27.

[f] The wall reaction rate constants (58 - 62) are for 4 cm spherical vessels coated with boric acid. No estimates of uncertainty are given, as the values of the parameters depend critically on many factors (see text).

Table II. Coefficients for Computing Specific Heat Capacities, $\{C_{v_i}\}$, and Specific Enthalpies, $\{h_i\}$, for the H_2-O_2 System

Species	$c_{v_i}^{(0)}$	$c_{v_i}^{(1)}$	$h_i^{(0)}$	$h_i^{(1)}$
H	2.981	0	52,580	0.6778
HO_2	8.566	8.099 (-4)	5,050	-0.6415
H_2	4.791	6.361 (-4)	0	0
O_2	5.726	5.512 (-4)	0	0
H_2O	6.495	1.386 (-3)	-583,200	-0.7126
O	2.970	3.452 (-5)	34,520	-0.0100
OH	5.071	4.965 (-4)	9,650	-0.4579
H_2O_2	8.465	4.198 (-3)	-33,300	-0.7768
O_3	9.706	7.464 (-4)	34,400	0.0291

Table III. Mechanism for the Slow Reaction Between the Second and Third
Explosion Limits Indicated by Sensitivity Analysis

Reaction Number[a]	Reaction	Reason for Importance
2	$H + HO_2 \longrightarrow H_2 + O_2$	HO_2-containing
6	$H + H_2O_2 \longrightarrow H_2 + HO_2$	HO_2-containing
7	$H + H_2O_2 \longrightarrow H_2O + OH$	H_2O_2 — H_2O pathway
11	$H + O_2 \longrightarrow OH + O$	chain-branching
12	$H + O_2 + M \longrightarrow HO_2 + M$	chain-terminating
13	$2 HO_2 \longrightarrow H_2O_2 + O_2$	HO_2 — H_2O_2 pathway
14	$H_2 + HO_2 \longrightarrow H_2O_2 + H$	HO_2 — H_2O_2 pathway
20	$H_2 + O \longrightarrow H + OH$	chain-branching
23	$O + H_2O_2 \longrightarrow OH + HO_2$	H_2O_2 — H_2O pathway
26	$H_2 + OH \longrightarrow H_2O + H$	H_2O producing
28	$OH + H_2O_2 \longrightarrow H_2O + HO_2$	HO_2-containing
34	$H_2 + O_2 \longrightarrow H + HO_2$	chain-initiating
35	$H_2 + O_2 \longrightarrow 2 OH$	chain-initiating
40	$H_2O_2 + M \longrightarrow 2 OH + M$	chain-restoring
45	$H_2 + HO_2 \longrightarrow H_2O + OH$	HO_2-containing

[a] Reaction numbers correspond to those given in Table I.

Table IV. Mechanism for the Second Explosion Limit Indicated by Sensitivity Analysis

Reaction Number[a]	Reaction	Reason for Importance
1	$2H + M \longrightarrow H_2 + M$	H-containing
2	$H + HO_2 \longrightarrow H_2 + O_2$	H-containing
3	$H + HO_2 \longrightarrow H_2O + O$	H-containing
4	$H + HO_2 \longrightarrow 2OH$	H-containing
5	$H + H_2O \longrightarrow H_2 + OH$	H-containing
8	$H + O + M \longrightarrow OH + M$	H-containing
10	$H + OH + M \longrightarrow H_2O + M$	H-containing
11	$H + O_2 \longrightarrow OH + O$	chain-branching
12	$H + O_2 + M \longrightarrow HO_2 + M$	chain terminating
20	$H_2 + O \longrightarrow H + OH$	chain-branching
24	$OH + O \longrightarrow H + O_2$	Reverse of Reaction 11
26	$H_2 + OH \longrightarrow H_2O + H$	H-containing
35	$H_2 + O_2 \longrightarrow 2OH$	chain-initiating

[a] Reaction numbers correspond to those given in Table I.

Table V.   Insignificant Reactions for the H_2-O_2 System Indicated by
Sensitivity Analysis

Reaction Number[a]	Reaction	Reason for U_{ni} importance
17	$OH + HO_2 \longrightarrow H_2O_2 + O$	other products more likely
29	$2\,OH \longrightarrow H + HO_2$	radical-radical
30	$2\,OH \longrightarrow H_2 + O_2$	radical-radical
32	$2\,OH + M \longrightarrow H_2O_2 + M$	radical-radical
33	$OH + M \longrightarrow O + H + M$	endothermic
38	$H_2 + M \longrightarrow 2\,H + M$	endothermic
42	$O_2 + M \longrightarrow 2\,O + M$	endothermic
44	$O_2 + OH \longrightarrow HO_2 + O$	endothermic
46	$H_2O + OH \longrightarrow H_2 + HO_2$	endothermic
48	$H_2O + O_2 \longrightarrow H_2O_2 + O$	endothermic
52	$2\,O_2 \longrightarrow O + O_3$	endothermic
54	$OH + O_2 \longrightarrow H + O_3$	endothermic

[a] Reaction numbers correspond to those given in Table I.

Figure Captions

Figure 1. Illustration of the variation of the reaction rate as a function of the initial pressure of H_2 and O_2. P_1, P_2, and P_3 denote the first, second and third explosion limit pressures, respectively. $T \cong 750^\circ K$.

Figure 2. Explosion limits of a stoichiometric H_2-O_2 mixture in a spherical KCl-coated vessel of 7.4 cm diameter. In this and in subsequent figures the explosion limit pressure is the sum of the initial partial pressures of H_2 and O_2 which cause explosion at a particular temperature. No diluent is present. The dotted lines indicate that the boundaries are uncertain. (After reference 21, p. 9.)

Figure 3. Concentration profiles for the calculation described in Section III. $T = 700^\circ K$, P_{init} = 320 torr, stoichiometric mixture of H_2 and O_2, no diluent present. This figure, as well as Figures 6, 7, 8 and 9 were produced directly from the differential equation solver mesh points. Straight lines are drawn between the irregularly spaced points.

Figure 4. Plot of a typical integrand for a sensitivity coefficient for the sample calculation described in Section III. This plot is for the coefficient $\partial[H]/\partial k_{20}$ evaluated at 10^3 sec. The scale is expanded for the final 2% of the interval. The shaded area under the curve illustrates the contribution to the integral.

Figure 5. Same as Figure 2, except that the results of a number of isothermal kinetic calculations are displayed as well. The notation is as follows: S denotes slow reactions, which according to the calculations take more than 10 seconds to achieve 50% completion; M refers to moderately fast reactions, which take between 0.5 and 10 seconds to reach 50% completion; and F refers to fast reactions, which require fewer than 0.5 seconds to reach 50% completion. The notation R refers to situations for which large concentrations of reactive radicals H, O and OH are observed. Such reactions are generally explosive. N refers to smaller concentrations of the reactive radicals and larger concentrations of the species HO_2 and H_2O_2. Such reactions are generally slower (S or M) and display non-explosive behavior.

Figure 6. Same as Figure 3, except that only the 15 most sensitive reactions are used as the model. O_3 does not appear since it does not enter into any of these reactions.

Figure 7. (a) Concentration profiles for a calculation carried out at $T = 825°K$, $P_{init} = 320$ torr, Stoichiometric mixture of H_2 and O_2, no diluent present. Non-explosive behavior shown.

(b) Same as (a), except that $T = 840°K$. A delayed explosion is indicated.

(c) Same as (a), except that $T = 875°K$. Explosive behavior is indicated.

Figure 8. Concentration profiles for a calculation carried out at

$T = 993°K$, $P_{init} = 64$ torr. Nitrogen (64 torr) is present as

a diluent. This calculation is for the experiment described in

reference 40. The induction time is obtained from the rapid

decrease in H_2 pressure; our estimate is 5×10^{-4} sec.

Figure 9. Concentration profiles for the decomposition of H_2O_2. $T = 750°K$,

$P_{init(H_2O_2)} = 213$ torr. Argon (360 torr) is present as a

diluent. The concentrations of H, O and O_3 are very small and off

scale.

FIGURE 1

SLOW

FAST

3

2

1

Pressure (torr)

10^3

10^2

10

1

700   800

Temperature (°K)
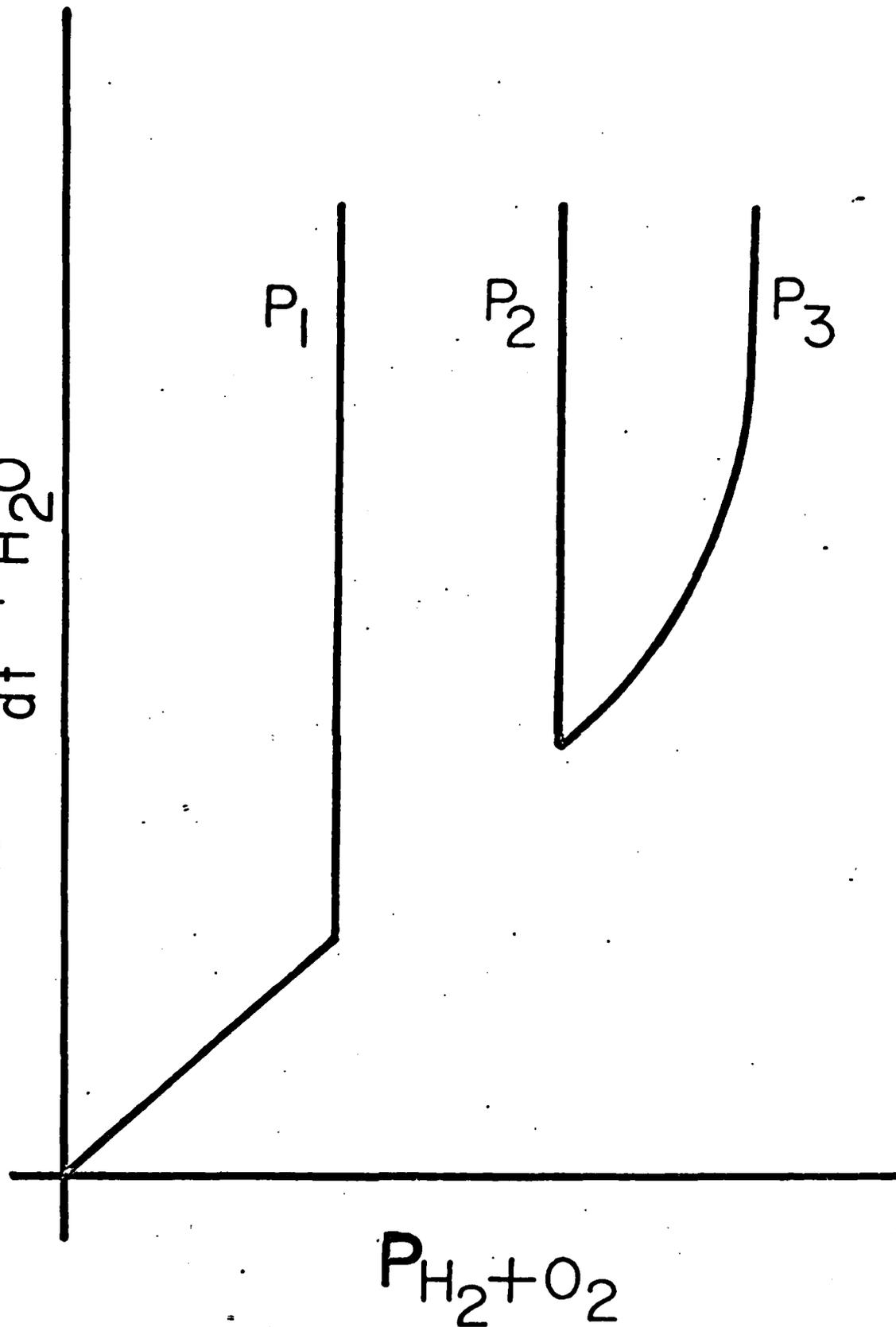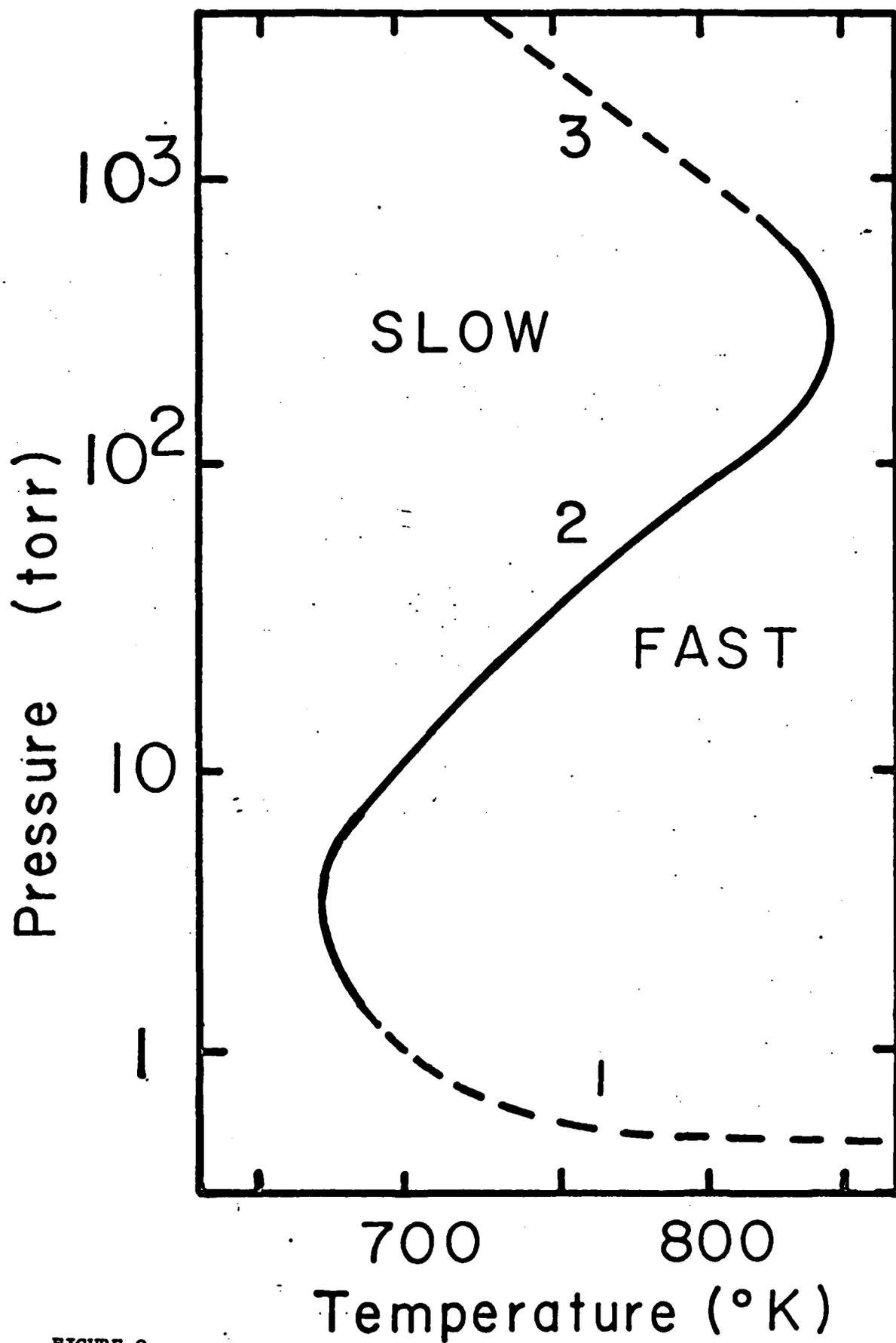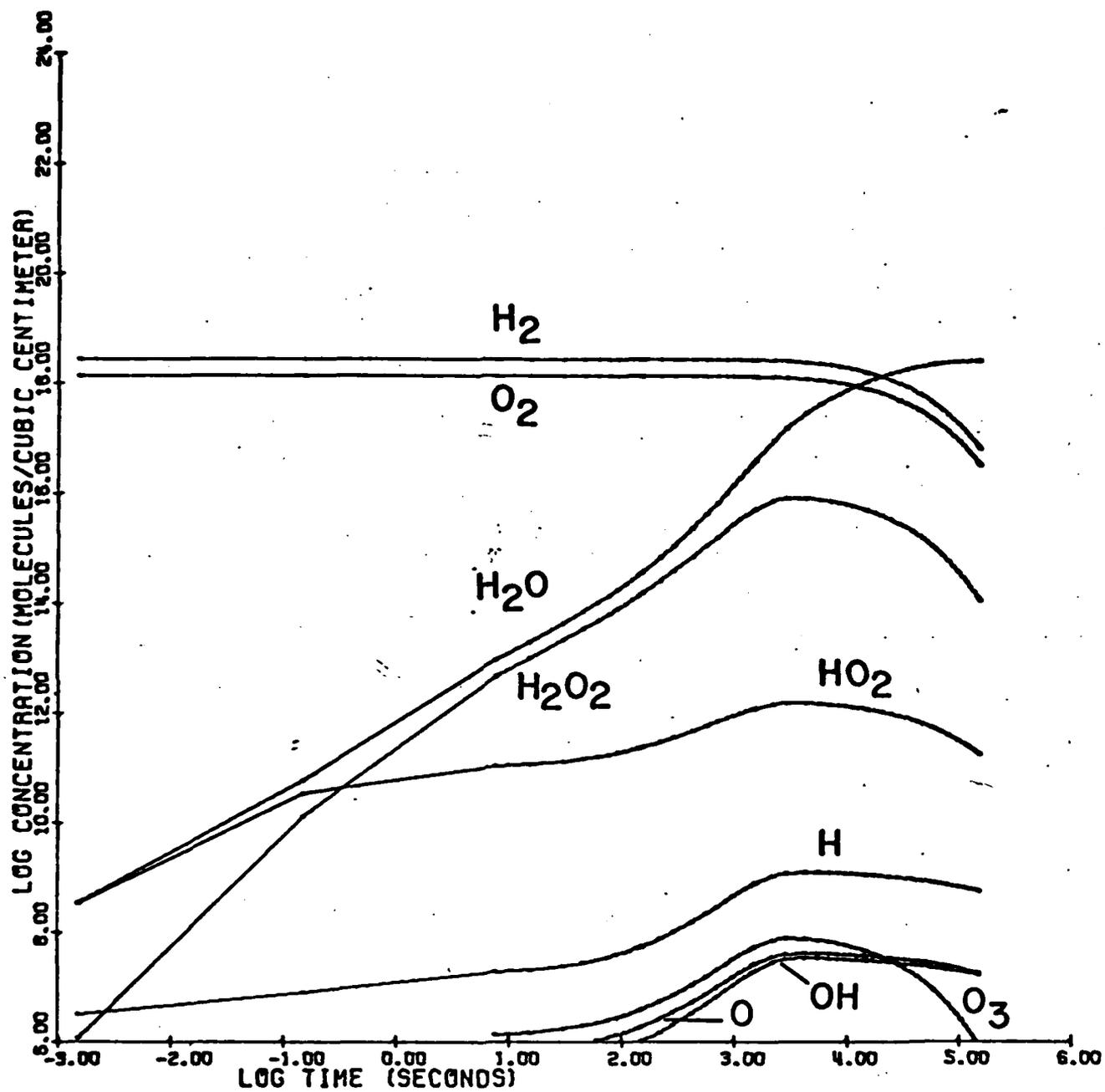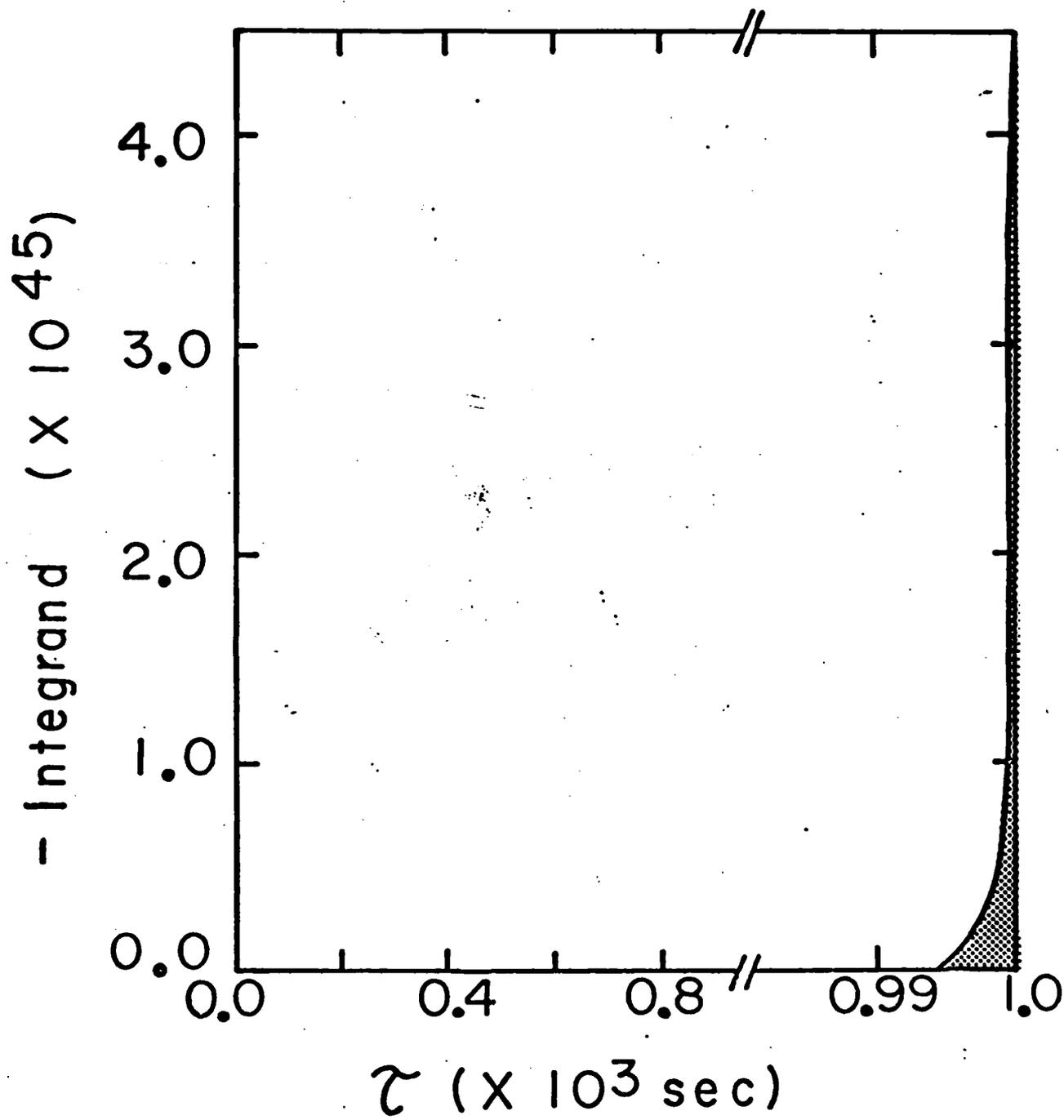
FIGURE 2

FIGURE 3

FIGURE 4
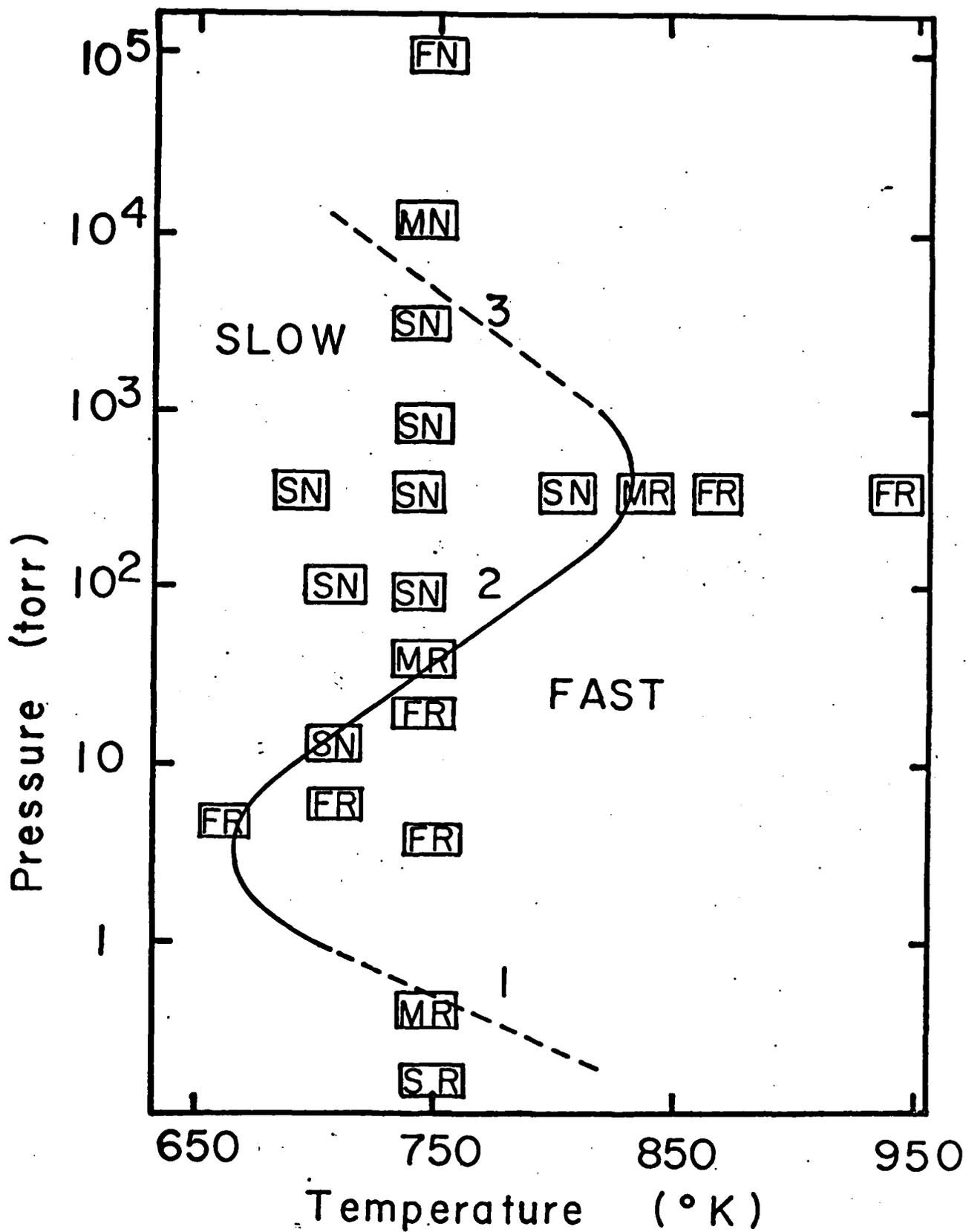
FIGURE 5
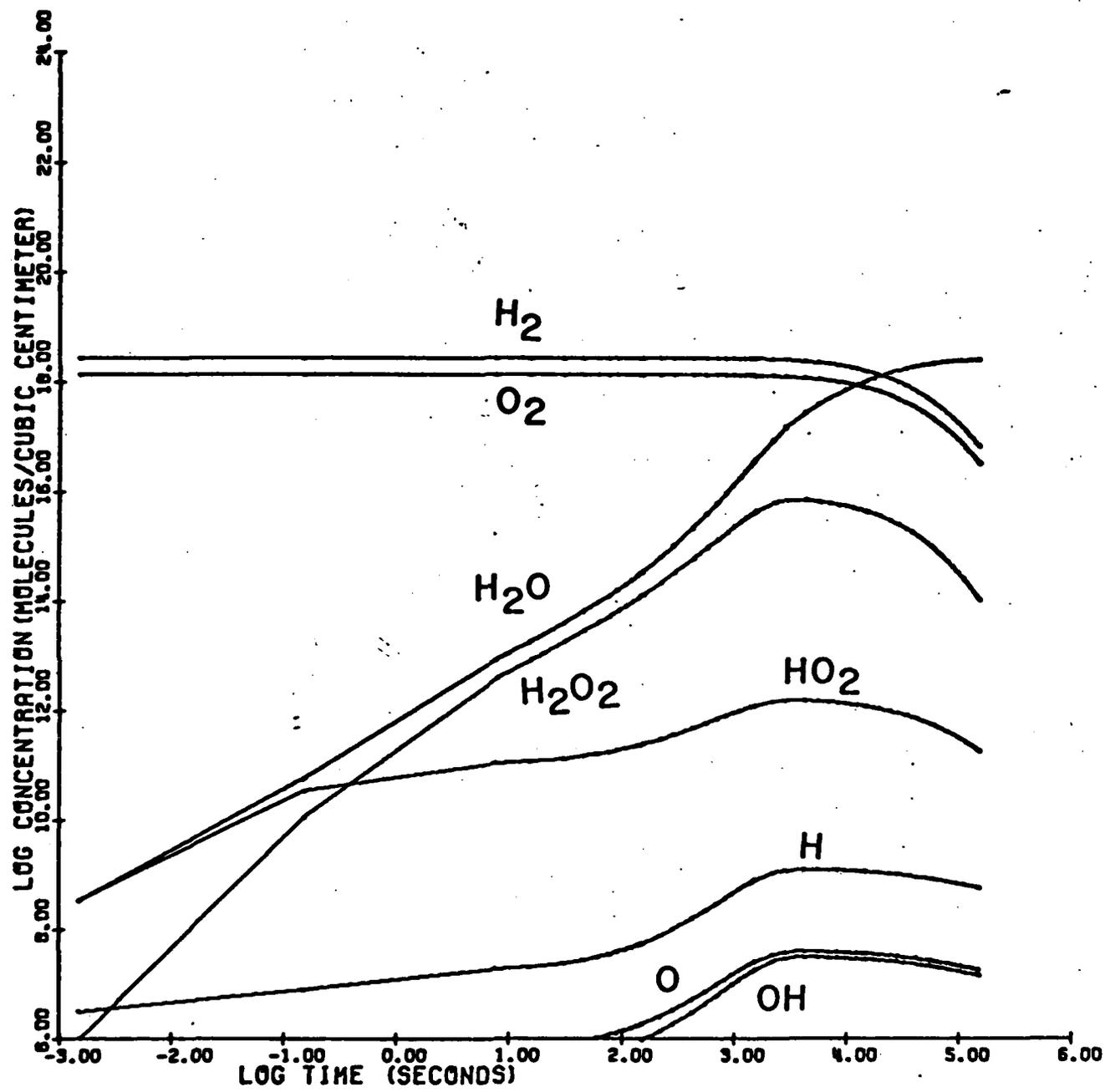
FIGURE 6
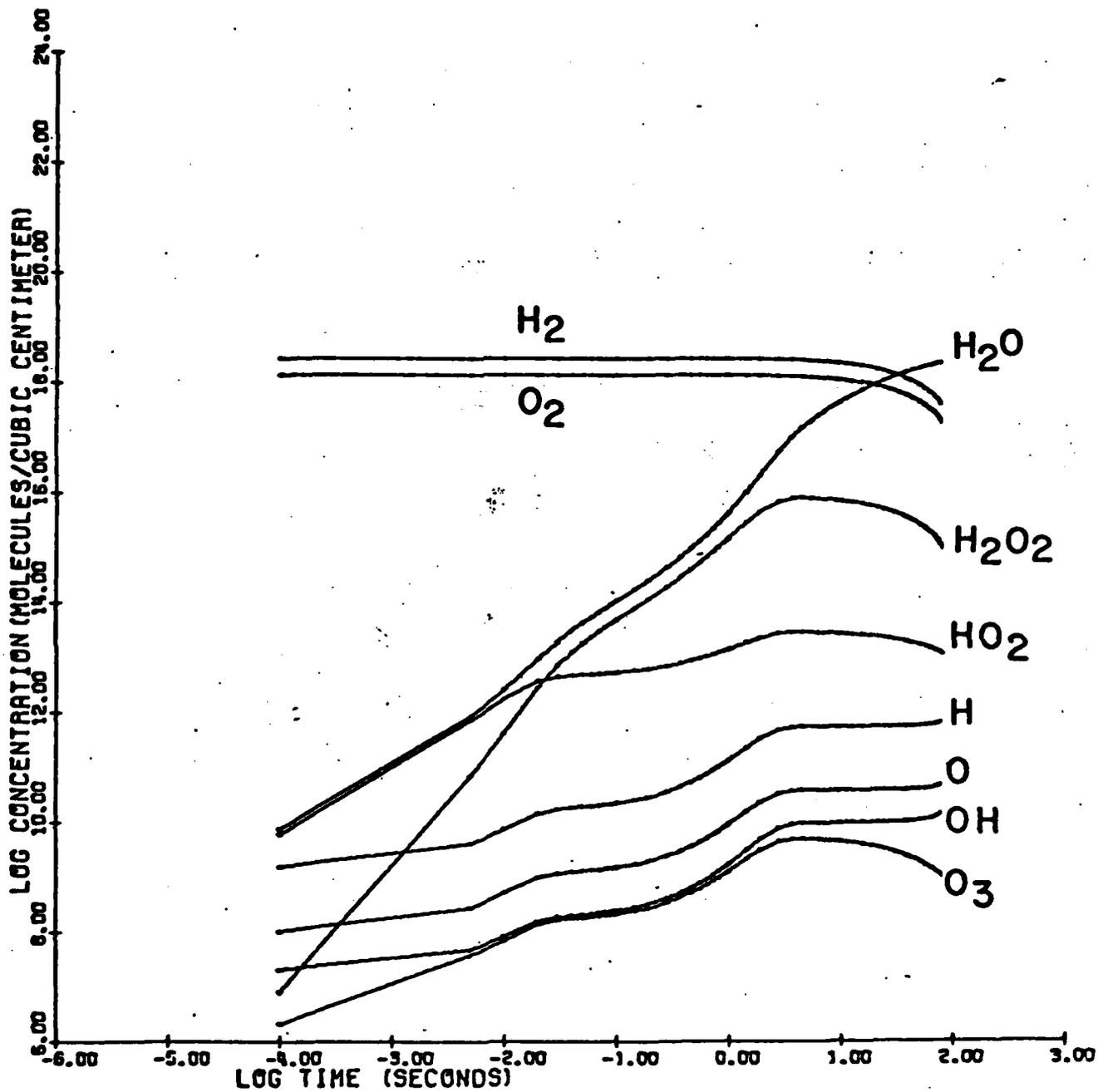
FIGURE 7a
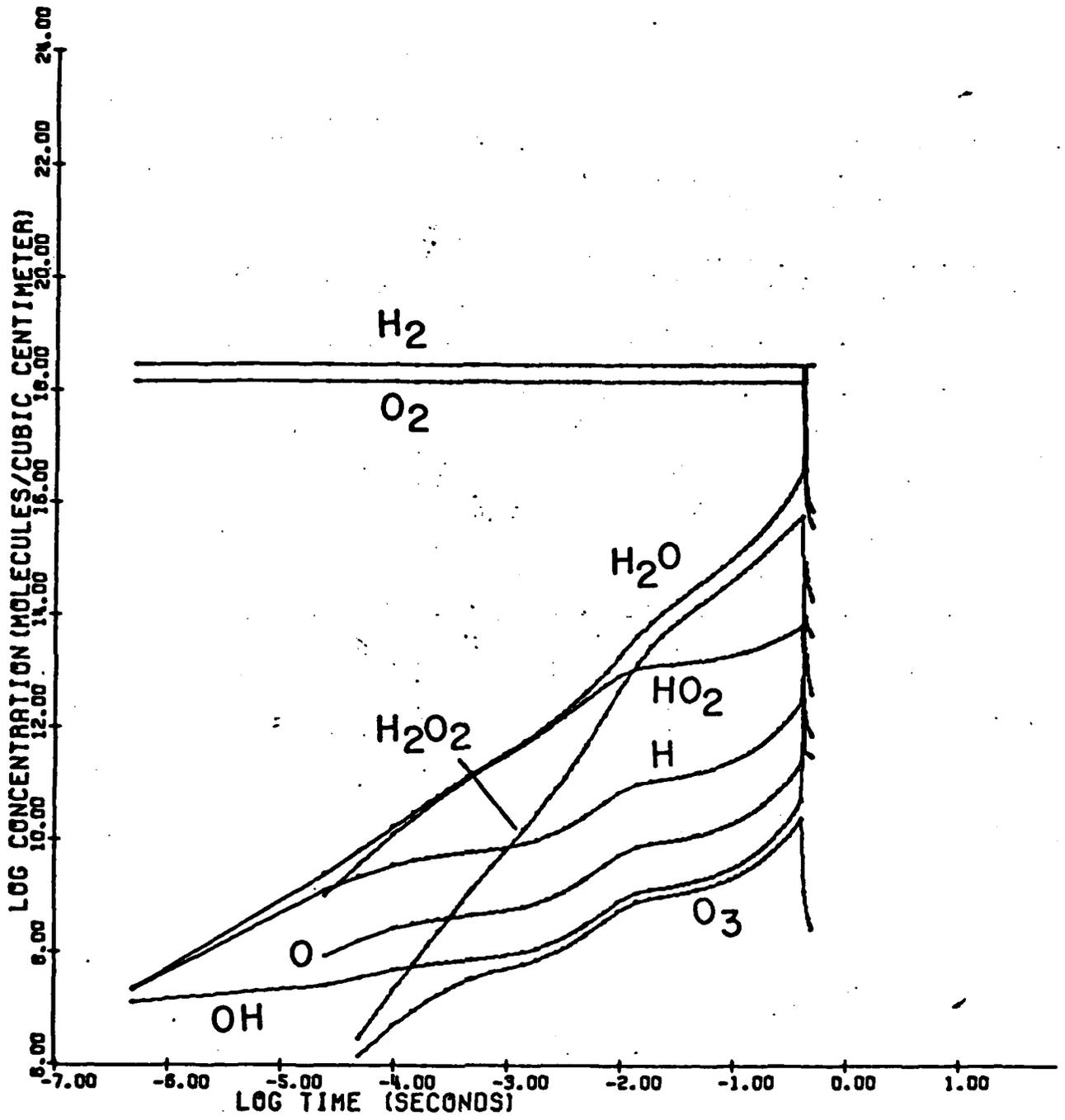
FIGURE 7b
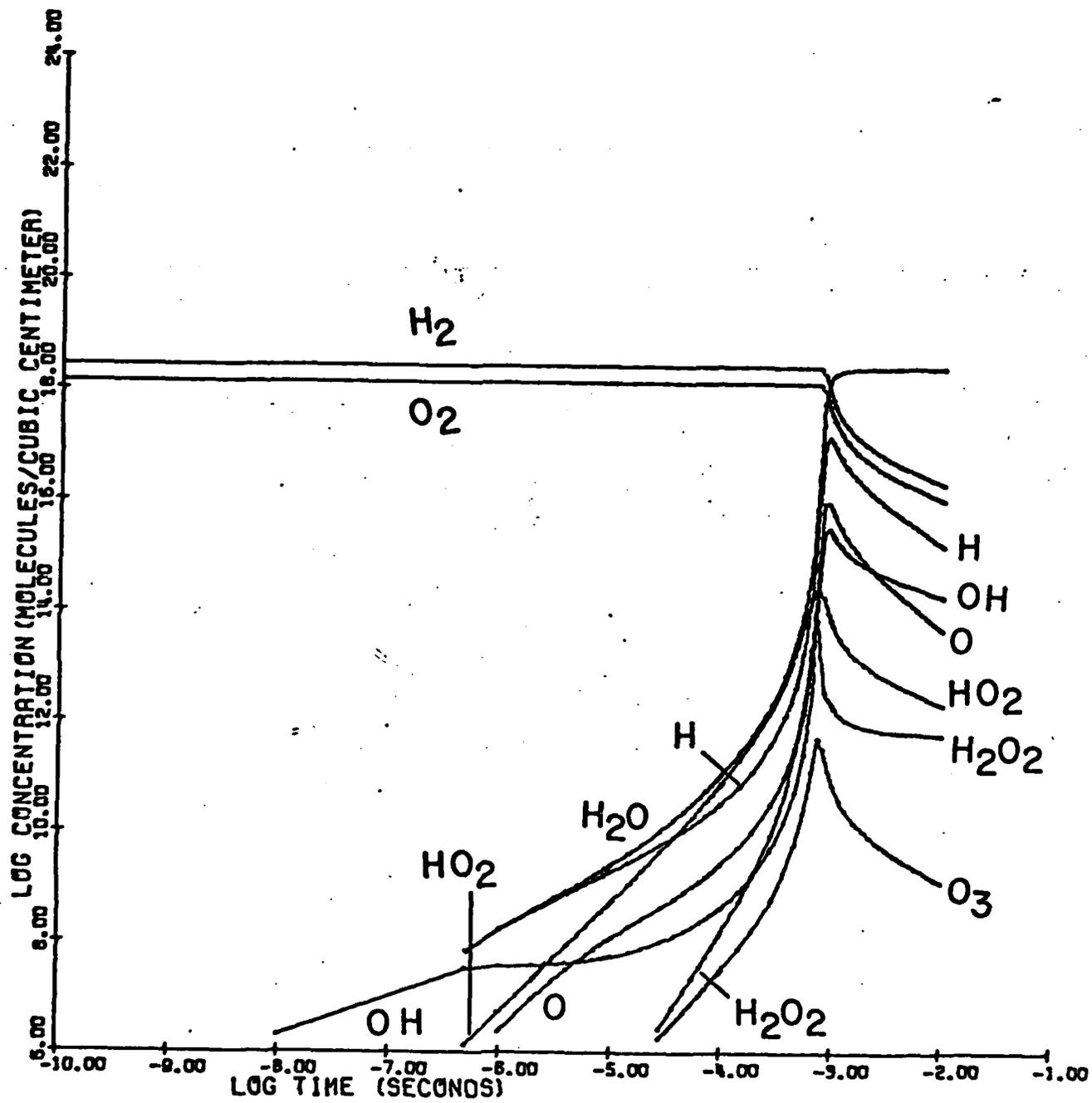
FIGURE 7c

FIGURE 8

FIGURE 9